iScience

CellPress
OPEN ACCESS

Article

A nano erythropoiesis stimulating agent for the treatment of anemia and associated disorders

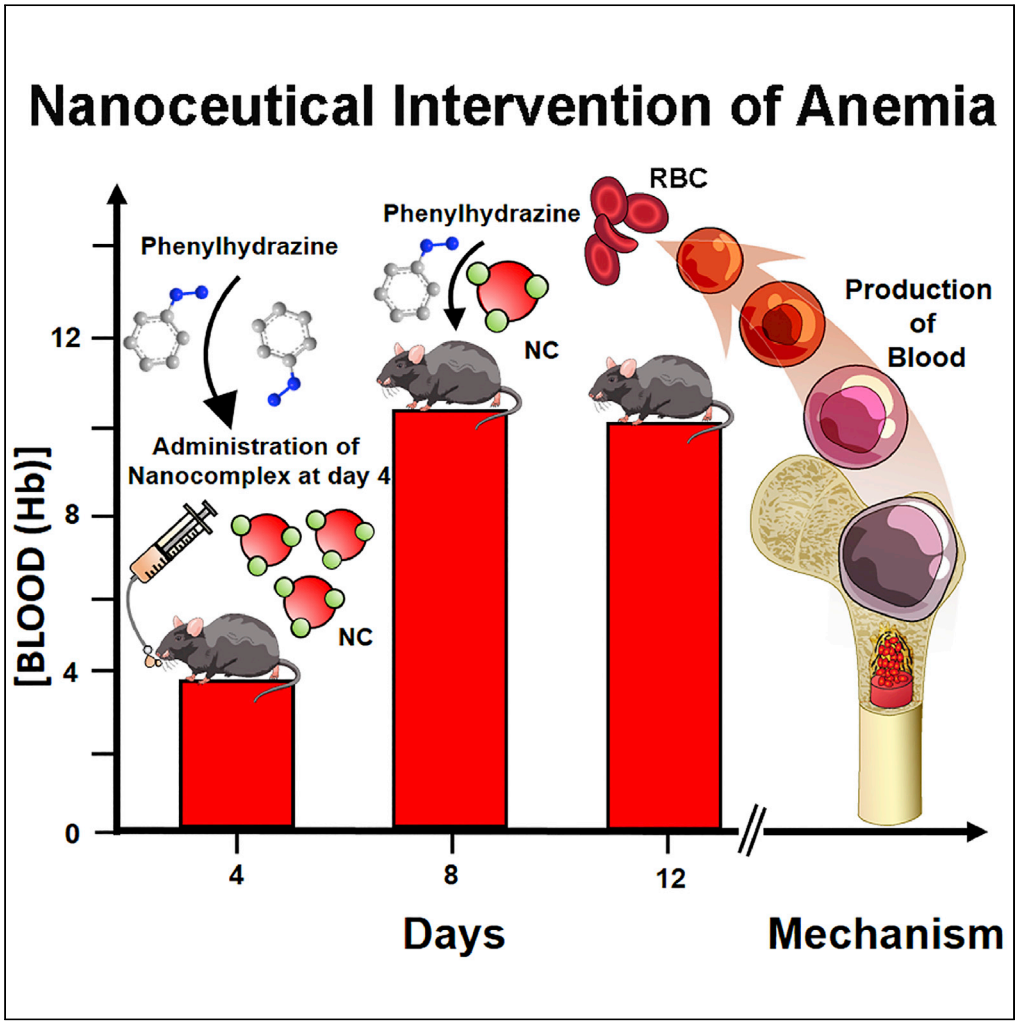

Monojit Das, Susmita Mondal, Ria Ghosh, ..., Jayanta Kumar Kundu, Aniruddha Adhikari, Samir Kumar Pal

jayantak62@gmail.com (J.K.K.)
aniruddhacbe@ucla.edu (A.A.)
skpal@bose.res.in (S.K.P.)

Highlights

Mn-citrate nanocomplex shows prophylactic and therapeutic effect in anemia of inflammation

It acts as erythropoiesis-stimulating agent by initiating hypoxia-induced erythropoiesis

It ameliorates pro-inflammatory signaling cascade, the major cause of anemia progression

It protects erythrocytes from oxidative damages and prevents further destruction of RBCs

Das et al., iScience 25, 105021
September 16, 2022
https://doi.org/10.1016/j.isci.2022.105021

iScience

CellPress
OPEN ACCESS

Article

A nano erythropoiesis stimulating agent for the treatment of anemia and associated disorders

Monojit Das,[1,2] Susmita Mondal,[3] Ria Ghosh,[3,4] Pritam Biswas,[5] Ziad Moussa,[6] Soumendra Darbar,[7] Saleh A. Ahmed,[8,9] Anjan Kumar Das,[10] Siddhartha Sankar Bhattacharya,[2] Debasish Pal,[2] Asim Kumar Mallick,[11] Prantar Chakrabarti,[12] Jayanta Kumar Kundu,[1,*] Aniruddha Adhikari,[13,*] and Samir Kumar Pal[2,3,14,*]

SUMMARY

The usual treatment for anemia and especially for anemia of inflammation (also called anemia of chronic disease) is supportive care with the target of improving the lifestyle of the patients. There is no effective medication to date for proper management. As the inflammation, erythropoiesis, and oxidative stress are the major concerns in this case, it inspired us to use a nano-erythropoietin stimulating agent (nano-ESA) made up of a nano-complex of manganese and citrate (Mn-citrate nano-complex), which has been hypothesized to have excellent antioxidant and anti-inflammatory mechanisms. Single oral dose of the nano-ESA efficiently prevented the onset of anemia as well as led to recovery from anemia in our phenylhydrazine (PHz)-intoxicated C57BL/6J mice model of anemia without any toxicological side effects. These preliminary findings may pave the way for an affordable and safe clinical use of the nano-ESA as a rapid recovery medication of anemia, especially anemia of inflammation.

INTRODUCTION

Anemia, or low circulating erythrocyte (red blood cell, RBC) count, remains one of the severe public health concerns affecting ~2.36 billion people worldwide (i.e., one-third of the global population) (Nguyen et al., 2018). It is the prime cause of years lived with disability (YLD) for women and contributes to significant morbidity and mortality (Nguyen et al., 2018). The etiology of anemia is heterogeneous and can be attributed to several risk factors (i.e., nutritional deficiency, genetic disorder, cancer, hemorrhage, inflammation, and chronic diseases) that either shorten the physiological 120-day lifespan of human erythrocytes or cause inefficient erythropoiesis (Theurl et al., 2016; Sankaran and Weiss, 2015; Paulson, 2014). Researchers have tried to focus on a new regulator of erythropoiesis to alleviate anemia (Suragani et al., 2014). Among all, anemia of anemia of inflammation (often termed anemia of chronic diseases) and iron-deficiency anemia are most frequent and often co-exists in people living in the developing countries (Ganz, 2019). The iron deficiency anemia is prevalent in growing children, premenopausal and pregnant women worldwide, and usually treated with iron supplementation therapy (Pasricha et al., 2021; Camaschella, 2015, 2019; Farrell and Lamont, 1998). Au contraire, anemia of inflammation is common in adults, critically ill, and elderly population and has classically been associated with chronic systemic inflammatory disorders including rheumatoid arthritis (Song et al., 2013), inflammatory bowel disease (Kaitha et al., 2015), infections (i.e., tuberculosis and acquired immunodeficiency syndrome, AIDS) (Gil-Santana et al., 2019), hematologic cancers (Adamson, 2008), and paraneoplastic syndromes (Puthenparambil et al., 2010). Lately, anemia of inflammation has been identified as the major contributing risk factor for survival in many other patients, including those with chronic kidney disease (Hanudel et al., 2016), congestive heart failure (Opasich et al., 2005), chronic obstructive pulmonary disease (Boutou et al., 2015), cystic fibrosis (Fischer et al., 2007), and even diabetes (Erslev and Besarab, 1997; Thomas, 2007; Thomas et al., 2004; Faquin et al., 1992; Chatterjee et al., 2019, 2020). The pathogenesis includes involvement of cytokines and cells of the reticuloendothelial system that negatively affects iron homeostasis, proliferation of erythroid progenitor cells, production of erythropoietin (EPO), the primary hormone that propels erythropoiesis, and the survival of red blood cells (Weiss and Goodnough, 2005). The major and promising frontline therapeutic interventions for these types of anemia are blood transfusion or treatment with recombinant EPO that supports

[1]Department of Zoology, Vidyasagar University, Rangamati, Midnapore 721102, India

[2]Department of Zoology, Uluberia College, University of Calcutta, Uluberia, Howrah 711315, India

[3]Department of Chemical, Biological and Macromolecular Sciences, S. N. Bose National Centre for Basic Sciences, Block JD, Sector 3, Salt Lake, Kolkata 700106, India

[4]Department of Biochemistry, University of Calcutta, 35, Ballygunge Circular Road, Kolkata 700019, India

[5]Department of Microbiology, St. Xavier's College, 30, Mother Teresa Sarani, Kolkata 700016, India

[6]Department of Chemistry, College of Science, United Arab Emirates University, P.O. Box 15551, Al Ain, United Arab Emirates

[7]Research and Development Division, Dey's Medical Stores (Mfg.) Ltd, 62, Bondel Road, Ballygunge, Kolkata 700019, India

[8]Department of Chemistry, Faculty of Applied Science, Umm Al-Qura University, 21955 Makkah, Saudi Arabia

[9]Department of Chemistry, Faculty of Science, Assiut University, 71516 Assiut, Egypt

[10]Department of Pathology, Coochbehar Government Medical College and Hospital, Kotwali, Coochbehar 736101, India

[11]Department of Pediatric Medicine, Nil Ratan Sircar Medical College and Hospital, Kolkata 700014, India

Continued

erythropoiesis (Murphy et al., 2017; Docherty et al., 2018; Weiss and Goodnough, 2005; Goodnough et al., 2000; De Marchi et al., 1993; Means, 1994). However, both treatments have several drawbacks. Despite significant improvements in the blood transfusion process, unavailability of the required blood stock, hospitalization cost, possibility of transfusion transmitted diseases, and high mortality remain the cause of concern (Aapro and Link, 2008; Bennett-Guerrero et al., 2007; Brittenham et al., 2001). On the other hand, apart from the well-recognized problems of protein-based therapies (i.e., immunogenicity, storage, stability, cost, and route of administration), recombinant EPO in recent clinical trials have shown tumor promoting and prothrombotic activities (Churchill et al., 2007; Sinclair, 2013; Hu et al., 2016; Lippi et al., 2010). Therefore, it is of considerable interest to develop an alternative non-protein therapeutic intervention, preferably with good oral bioavailability that can simultaneously stimulate erythropoiesis and alleviate inflammatory responses to treat this debilitating clinical complication. In this regard, engineered nanomaterials could be of potential use due to their unique interactions with the biomolecules in the physiological milieu and tunable physicochemical, optical, and electromagnetic properties that significantly differs from other synthetic drug molecules because of the nanoscale dimension and consequent quantum effects. In the last two decades, various nanomaterials have demonstrated effectiveness in treatment of a plethora of diseases, including cancer, hepatic fibrosis, chronic kidney disease, diabetes, and neurodegenerative disorders (Adhikari et al., 2016, 2021a, 2021b; Hu et al., 2020; Zhang et al., 2018; Ding et al., 2021). Some of them even received United States Food and Drug Administration (US-FDA) approval for use in the clinical settings (Anselmo and Mitragotri, 2016; Bobo et al., 2016).

In this study, we introduce an erythropoiesis-stimulating agent (ESA) made up of an engineered nanomaterial having the potential to treat anemia of inflammation. The nano-ESA is eventually a spherical nanocomplex consisting of manganese and citrate (i.e., the Mn-citrate nano-complex) and have a diameter of ~2–5 nm. To the best of our knowledge, no precedence of nano-complex or nano-formulation that functions as ESA to increase erythropoiesis in anemic conditions is available in the contemporary literature. Here, we have synthesized the unique nano-complex, standardized the preparation procedure, and thoroughly characterized its physical, chemical, and optical properties using state-of-the-art electron microscopic and spectroscopic techniques. We evaluated therapeutic efficacy of the nano-ESA in the treatment of anemia using a suitable animal model (i.e., phenylhydrazine (PHz) intoxicated C57BL/6J mice). We have further explored the underlying molecular mechanism of therapeutic action of the nano-ESA that involved synergistic upregulation of EPO synthesis, reduction of inflammatory responses, and intracellular redox buffering.

RESULTS

Physicochemical characteristics of the nano-complex

The transmission electron micrograph (TEM) of the synthesized nanocomplex (Figure 1A) shows the manganese citrate nano-complex (Mn-citrate NC) to be spherical in shape, having a monomodal size distribution. The high-resolution (HR)-TEM of a single particle (Figure 1B) confirms the crystallinity with an inter-fringe lattice distance of ~0.25 nm corresponding to the 330 plane of the α-phase metallic Mn. Size distribution histogram (Figure 1C) shows the homogeneity in size of Mn-citrate NC. Selected area electron diffraction (SAED) further confirms the crystallinity of the material (Figure 1A, inset). Figure 1D shows the powdered X-ray diffraction analysis of the nanomaterial. The diffraction peaks could be assigned to the α-phase metallic Mn or MnO. This indicates the presence of a metallic core made up of α-Mn, and the surface Mn formed oxide with the citrate. This provides a unique structure to a commonly available metal that has not been characterized until date.

The absorbance spectra showed ligand to metal charge transfer (LMCT) bands around 280 and 320 nm, and d-d transition bands around 430 and 510 nm, lifted by forbidden Jahn-Tellar distortion (Figures S1, A and A, inset). The appearance of LMCT band further confirms the presence of Mn-citrate bond at the surface of the nanocomplex. Figure S1B shows the emission peaks when excited at the absorption bands. Figure S1C shows the corresponding excitation spectra that complement the absorption bands.

The nano-complex in prevention of anemia

Next, we evaluated the efficacy of the nanomaterial for the treatment of anemia in a preclinical animal model of anemia. Here, animals were administered phenylhydrazine (PHz), a known hemolytic agent for induction of anemia. The Mn-citrate NCs were simultaneously treated (co-treatment) in order to test their role as a preventive medicine. At first, we monitored the effect of Mn-citrate NC on hemoglobin (Hb) level

[12]Department of Hematology, Vivekananda Institute of Medical Sciences, Kolkata 700026, India

[13]Department of Chemical and Biomolecular Engineering, UCLA Samueli School of Engineering, University of California, at Los Angeles (UCLA), Los Angeles, USA

[14]Lead contact

*Correspondence: jayantak62@gmail.com (J.K.K.), aniruddhacbe@ucla.edu (A.A.), skpal@bose.res.in (S.K.P.)

https://doi.org/10.1016/j.isci.2022.105021

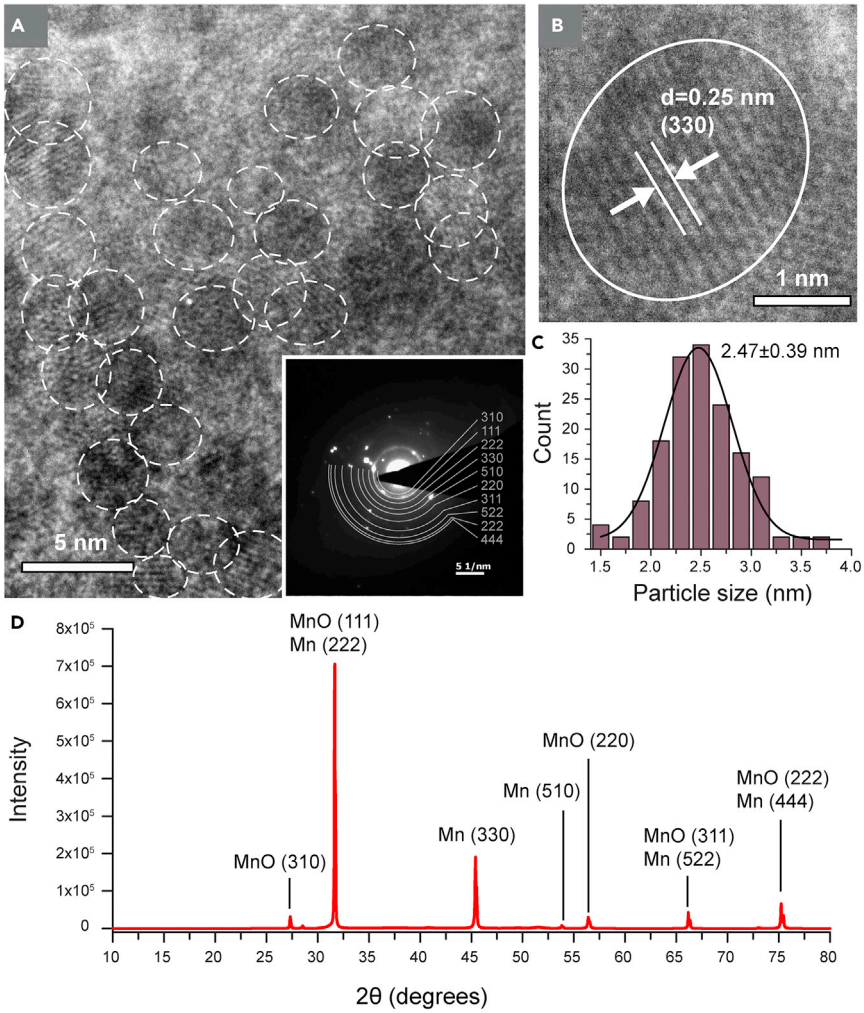

Figure 1. Physicochemical characteristics of Mn-citrate nanocomplex

(A) TEM of the complex. Inset shows SAED pattern of the same.

(B) HR-TEM of a single particle.

(C) Size distribution.

(D) XRD of the nanocomplex shows signature of metallic Mn as well as MnO crystal. See also Figure S1.

for 14 days at regular intervals after co-treatment with single intraperitoneal injection (i.p.) of PHz and oral administration of Mn-citrate NC.

Mice treated with PHz alone developed anemia within first 6 h of administration (Hb: 9.9 $\pm$ 0.30 g dL^{-1}; $p < 0.0001$, $F(4, 40.29) = 337.3$, one-way ANOVA, compared to control, Hb:13.64 $\pm$ 0.34 g dL^{-1}) (Figure 2A). Drastic reduction of Hb in PHz-treated mice confirmed the induction of severe hemolysis and anemia due to PHz intoxication. On the other hand, in co-treated mice, Hb level was within the normal range (Hb: 13.05 $\pm$ 0.35 g dL^{-1}, $p < 0.0001$, one-way ANOVA), which was much higher than the PHz intoxicated mice. Figures 2A and 2B further depicts that on day 4 the Hb level reached its lowest in the PHz-intoxicated animals. Whereas, the animals co-treated with PHz + Mn-citrate NC never developed anemia. The animals treated with Mn-citrate alone maintained normal Hb level throughout the experimental period.

We continued monitoring the Hb level up to day 14. There was no promising increase in Hb level of the PHz-intoxicated mice on day 8 (Hb: 8.07 $\pm$ 0.63 g dL^{-1}; $p < 0.0001$, $F(4, 42.83) = 315.4$, one-way ANOVA, compared with control Hb: 13.29 $\pm$ 0.47 g dL^{-1}), whereas, the mice co-treated with PHz + Mn-citrate NC (Hb:13.11 $\pm$ 0.51 g dL^{-1}, $p < 0.0001$, one-way ANOVA) prevented the Hb-loss and recovered normal

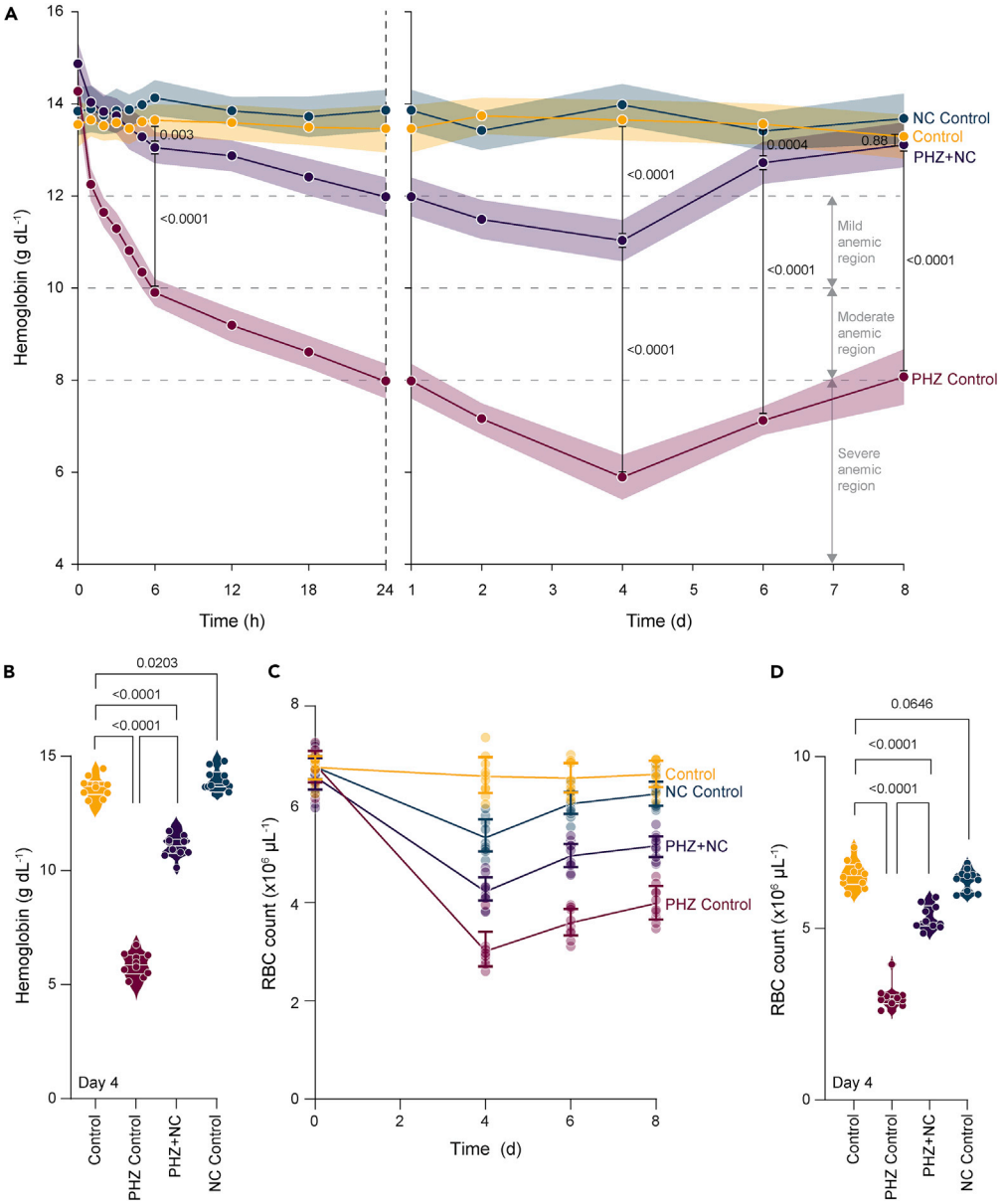

Figure 2. Efficacy of Mn-citrate nanocomplex in protection of anemia in animal model

(A) Hemoglobin concentration throughout the study. Single dose of nanocomplex was able to prevent anemia development. (B) Hemoglobin concentration on day 4.

(C) RBC count throughout the study. NCs successfully prevented the progressive decrease of RBCs.

(D) RBC count on day 4. Data are expressed as mean ± SD (n = 10). Individual data points are represented as colored circles (n = 10). One-way ANOVA followed by correction of false discovery rate (post hoc FDR: 2-stage step up method of Benjamini, Krieger, and Yekutieli) for multiple comparisons was performed for comparison between multiple groups. See also Figure S3.

Hb-level (Figure 2A). Cumulatively, these results suggest that Mn-citrate NC effectively prevents the progression of anemia induced by PHz administration. We still monitored the Hb level up to day 14 to know the recovery period of PHz-induced anemia in mice model (Figure S3A). On day 10, mice treated with only PHz showed slightly increased Hb level (Hb: 10.67 ± 0.34 g dL^{-1}; $p < 0.0001$, $F(4, 39.81) = 216.4$, one-way ANOVA, compared with control Hb:14.05 ± 0.49 g dL^{-1}) but still within the range of mild anemic region. The Hb level of PHz-intoxicated mice reached to normal condition (Hb: 13.97 ± 0.27 g dL^{-1}; $p = 0.9314$, $F(4, 37.95) = 16.2$, one-way ANOVA, compared with control Hb:13.98 ± 0.27 g dL^{-1}) on day 14. We also

measured the RBC count at regular intervals up to 14 days (Figure S3B). Significant decrease in RBC count was observed in the mice treated with PHz alone (RBC: 3.01 ± 0.36 10^6 μL^{-1}; $p < 0.0001$, $F(4, 42.86) = 266.8$, one-way ANOVA) compared with the control (RBC: 6.57 ± 0.40 10^6 μL^{-1}) on day 4 (Figures 2C and 2D). Co-treated mice showed remarkably higher RBC count (RBC: 5.32 ± 0.35 10^6 μL^{-1}) in comparison to PHz-intoxicated mice ($p < 0.0001$, one-way ANOVA). There was no significant increase in RBC count in PHz-intoxicated mice on day 8 (RBC: 3.98 ± 0.35 10^6 μL^{-1}; $p < 0.0001$, $F(4, 43.62) = 224.0$, one-way ANOVA). The co-treated group showed similar trend to the Hb level and reached almost normal RBC count (RBC: 6.21 ± 0.31 10^6 μL^{-1}) on day 8 (Figure 2C). We continued monitoring RBCs count up to day 14 to validate the recovery duration of PHz-induced anemia in mice model (Figure S3B). The PHz-intoxicated mice could not reach the normal level but showed a slightly increased RBC count (RBC: 5.13 ± 0.34 10^6 μL-1; $p < 0.0001$, $F(4, 43.61) = 94.34$, one-way ANOVA) compared with the control (RBC: 6.51 ± 0.29 10^6 μL^{-1}) on day 10. And the mice treated with only PHz reached its normal RBC count (RBC: 6.66 ± 0.25 10^6 μL^{-1}; $p = 0.1860$, $F(4, 43.38) = 4.196$, one-way ANOVA) compared with the control (RBC: 6.49 ± 0.29 10^6 μL^{-1}) on day 14. On the other hand, mice co-treated with PHz + citrate demonstrated same recovery period as PHz-intoxicated mice. Treatment with citrate failed to normalize the Hb level and RBC count (Figure S3) rapidly, confirming the observed effects solely due to the conjugated nanocomplex.

Next, to evaluate the physical features of RBCs, we investigated other RBC indices like mean corpuscular volume (MCV), mean corpuscular hemoglobin concentration (MCHC), mean cell hemoglobin (MCH), hematocrit (HCT) value etc. (Table S1). We found significantly increased MCV in PHz-only-treated mice (MCV: 107.2 ± 13.11 fL; $p < 0.0001$, $F(5, 18.31) = 24.57$, one-way ANOVA) compared with the control mice (MCV: 62.50 ± 5.19 fL) on day 4. Co-treatment with PHz + Mn-citrate NC showed remarkably improved MCV (66.97 ± 6.10 fL) in comparison to PHz-intoxicated mice ($p < 0.0001$, one-way ANOVA). PHz-intoxicated mice demonstrated notably lower MCHC (MCHC: 18.58 ± 2.18 g dL^{-1}; $p < 0.0001$, $F(5, 28.17) = 49.01$, one-way ANOVA) compared with control (MCHC: 33.60 ± 2.14 g dL^{-1}). PHz + Mn-citrate NC co-treated mice maintained MCHC within the normal range (MCHC: 31.15 ± 1.91 g dL^{-1}) compared with PHz-intoxicated untreated mice ($p < 0.0001$, one-way ANOVA). On the other hand, we did not observe any significant difference in case of MCH between groups ($p = 0.7042$, $F(5, 23.64) = 0.5947$, one-way ANOVA). Mice treated with PHz alone showed MCH value (MCH: 19.92 ± 3.47 pg) similar to that of control (MCH: 20.98 ± 2.01 pg, $p = 0.9707$, one-way ANOVA). Similarly, co-treatment with PHz + Mn-citrate NC demonstrated normal MCH value (MCH: 20.87 ± 2.11 pg) alike to that of control mice ($p = 0.9240$, one-way ANOVA). Administration of PHz alone significantly reduced hematocrit (Hct) value (Hct: 31.77 ± 1.76%, $p < 0.0001$, $F(5, 29.46) = 26.92$, one-way ANOVA) compared with control (Hct: 40.89 ± 1.95%). Reduction in Hct value further confirmed induction of PHz-induced hemolysis. Co-treatment with PHz + Mn-citrate NC showed slightly improved Hct value (Hct: 35.46 ± 1.94%) in comparison to the PHz-intoxicated mice ($p = 0.0064$, one-way ANOVA). No significant variation in any hematological parameter in mice treated with Mn-citrate NC alone during the entire experimental period indicated its hemocompatibility. The results altogether suggest that the Mn-citrate NC can efficiently prevent hemoglobin drop.

The nano-complex in treatment of anemia

The successful prevention of anemia by Mn-citrate NC motivated us to test its therapeutic potential against anemia. Here, instead of co-treatment the nano-complex was administered orally after induction of anemia. Effect of Mn-citrate NC on Hb level and RBC count was monitored at 2-day interval up to day 14, after treatment with single oral dose of Mn-citrate NC, once Hb level reached 6.19 ± 0.43 g dL^{-1} (compared with 13.62 ± 0.42 g dL^{-1} of control; $p < 0.0001$, $F(4, 44.47) = 922.9$, one-way ANOVA) and RBC count reached 3.19 ± 0.24 10^6 μL^{-1} (compared with 6.76 ± 0.30 10^6 $\mu L^{-1}$of control; $p < 0.0001$, $F(4, 43.69) = 489.1$, one-way ANOVA) on day 4 due to PHz intoxication (Figures 3A and 3B). As the results suggest, Mn-citrate NC was able to irreversibly increase both Hb level (10.27 ± 0.35 g dL^{-1}; $p < 0.0001$, $F(4, 40.88) = 678.9$, one-way ANOVA) and RBC count (5.03 ± 0.28 10^6 μL^{-1}; $p < 0.0001$, $F(4, 43.75) = 279.7$, one-way ANOVA) to normal range within 48 h. Furthermore, Mn-citrate-NC-treated mice showed higher Hb level (13.11 ± 0.56 g dL^{-1}; $p < 0.0001$, $F(4, 42.67) = 387.7$, one-way ANOVA) and RBC count (6.39 ± 0.28 10^6 μL^{-1}; $p < 0.0001$, $F(4, 43.57) = 213.6$, one-way ANOVA) compared with PHz-induced anemia model (Hb level: 8.16 ± 0.46 g $dL^{-1}$and RBCs: 4.05 ± 0.35 10^6 μL^{-1}) on day 8 (Figures 3C and 3D). So, these results confirm that Mn-citrate NC can effectively cure acute anemia in a short time. On the other hand, citrate-treated mice failed to recover from anemia same as PHz-only- intoxicated mice. In addition citrate-treated mice showed very low level of Hb (07.38 ± 0.41 g dL^{-1}; $p < 0.0001$) and RBC count (3.77 ± 0.28 10^6 μL^{-1}; $p < 0.0001$) on day 8 in

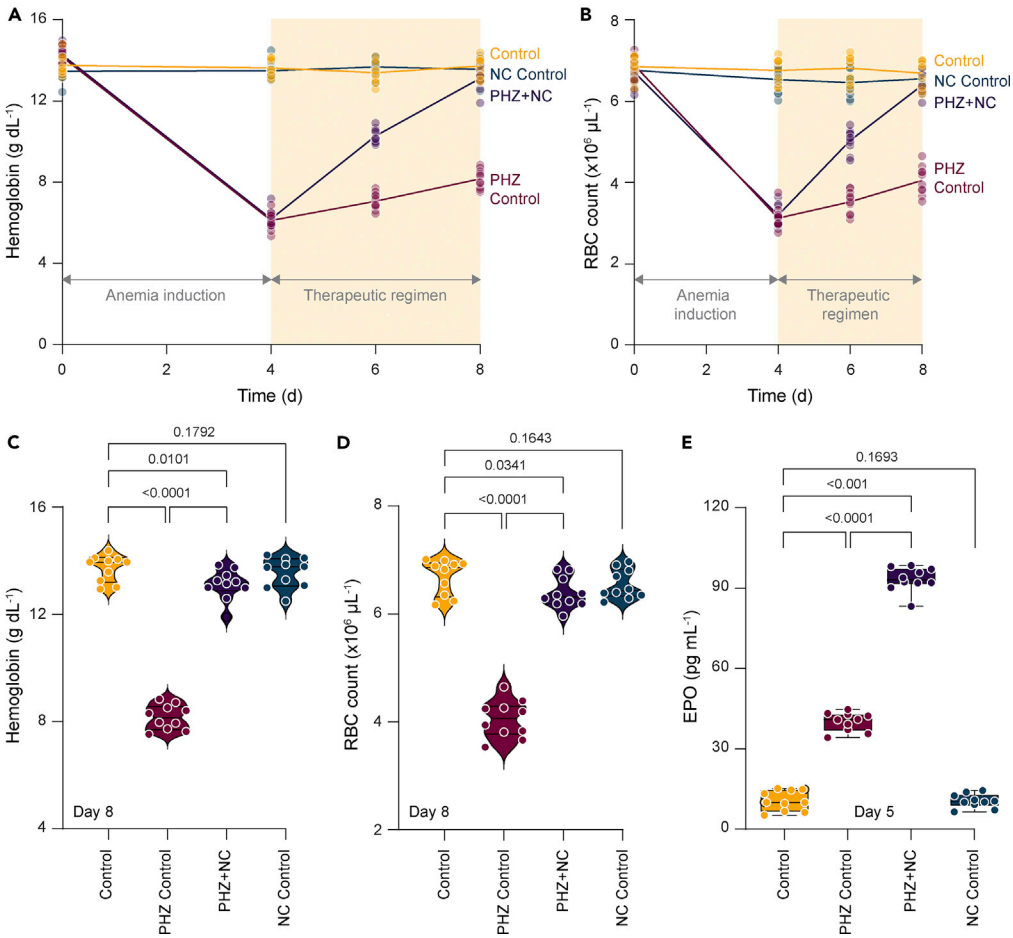

Figure 3. Efficacy of Mn-citrate nanocomplex as therapeutic medicine against anemia in animal model

(A) Hemoglobin concentration and (B) RBC count throughout the study. Single dose of nanocomplex was able to restore normal hemoglobin concentration and RBC count within 48 h.

(C) Hemoglobin concentration on day 8.

(D) RBC count on day 8.

(E) Serum erythropoietin (EPO) level on day 5. Data are expressed as mean ± SD (n = 10). Individual data points are represented as colored circles (n = 10). One-way ANOVA followed by correction of false discovery rate (post hoc FDR: two-stage step up method of Benjamini, Krieger, and Yekutieli) for multiple comparisons was performed for comparison between multiple groups. See also Figures S4 and S2.

comparison to control mice (Hb: 13.72 ± 0.41 g dL^{-1} and RBCs: 6.69 ± 0.32 10^6 μL^{-1}) (Figure S4). So, it also validates that treatment with citrate was unable to normalize the Hb level and RBC count (Figure S4), confirming the observed potential solely due to the conjugated nanocomplex.

The nano-complex in protection of hemolysis and prevention of splenomegaly

PHz administration induces severe type of hemolysis through its interaction with RBCs in mice (Spivak et al., 1973). To further understand the severity of hemolysis as well as structural changes of RBCs due to intoxication of PHz, we prepared blood smears on glass slides, stained with Leishman stain and evaluated under the microscope. We observed significantly low number of normal RBCs on blood smear in case of mice treated with only PHz compared with co-treated mice (Figures 4A and 4B). Furthermore, PHz-administered mice also showed many times higher proportion of hemolysis and abnormally shaped RBCs compared with mice treated with PHz and NC both (Figure 4A). Co-treated mice also demonstrated a very low number of WBCs on blood smear compared with mice treated with PHz alone (Figure 4A). We also performed complete blood count (CBC) including WBC count in cell counter to confirm the result. The CBC result showed PHz-treated mice had 2.37-fold higher WBCs in blood in comparison to control mice (Table S1). And PHz + NC-treated mice showed

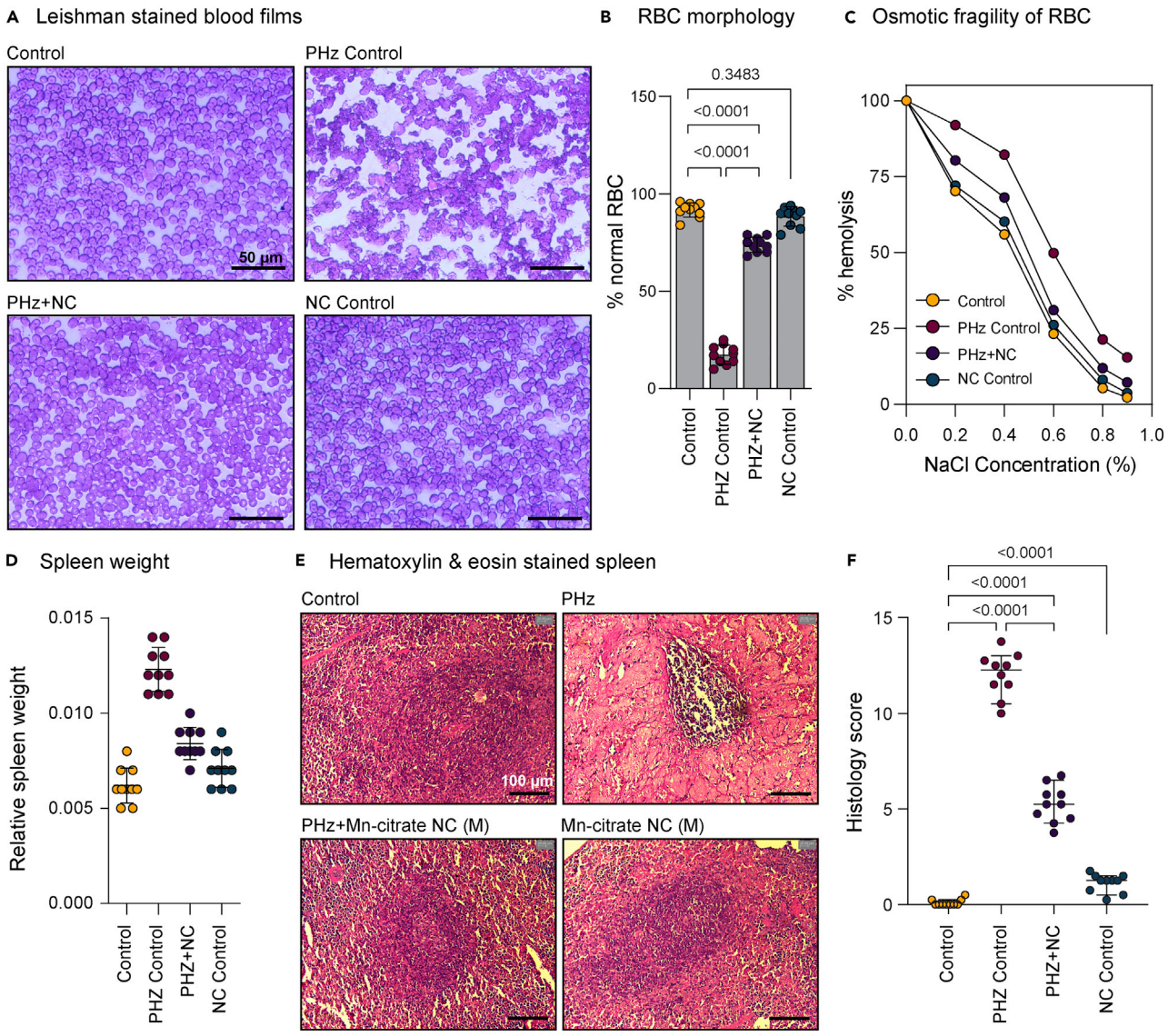

Figure 4. Potential of Mn-citrate nanocomplex in protection of blood cells and architecture of spleen

(A) Leishman-stained blood smear across all groups. Scale bar: 50 µm. (B) Percentage of normal RBCs. (C) Percentage of hemolysis.

(D) Relative spleen weight (E) H&E-stained spleen sections under microscope. Scale bar: 100 µm.

(F) Histology score. Data are expressed as mean ± SD (n = 10). Individual data points are represented as colored circles (n = 10). One-way ANOVA followed by correction of false discovery rate (post hoc FDR: two-stage step up method of Benjamini, Krieger, and Yekutieli) for multiple comparisons was performed for comparison between multiple groups. See also Figure S5.

almost normal level of WBCs in blood. This finding strongly indicates toward the activation of severe systemic inflammation in physiological milieu caused by PHz administration (Chmielewski and Strzelec, 2018). On the other hand, PHz can promote tremendous oxidative stress to the RBCs, leading to hemolysis of prone RBCs (Goldberg and Stern, 1977). So, we performed osmotic fragility test (OFT) on day 4 to measure erythrocyte resistance to hemolysis. The Figure 4C depicts the percentage of hemolysis of the RBCs of the co-treated mice is less considerable than that of the mice treated with only PHz. So, these results indicate that the NC increases the osmotic resistance of the RBCs of the mice treated with PHz. Hence, it can be reasonably concluded that Mn-citrate NC impedes the oxidative stress induced by PHz.

Previous studies also reported that severe splenomegaly (abnormal enlargement of spleen) was provoked due to the accelerated abnormal removal of damaged RBCs by resident macrophages in the

spleen, which may lead to substantial changes in the composition of the cell population in a short time and induction of inflammation in case of treatment with PHz (Rokushima et al., 2007; Nyakundi et al., 2019; Tolosano et al., 2002). So, we measured the relative spleen weight and analyzed the structural changes of hematoxylin and eosin (H&E)-stained spleen sections under microscope to assess the damage done to spleen. The relative spleen weight was 2-fold higher (Figure 4D) in PHz administered mice (Relative spleen weight: 0.0123 $\pm$ 0.0011; $p < 0.0001$, $F(3, 33.99) = 74.40$, one-way ANOVA) compared with control mice (relative spleen weight: 0.0062 $\pm$ 0.0009). At the same time, co-treatment with PHz + Mn-citrate NC in mice showed remarkably lower relative spleen weight (relative spleen weight: 0.0084 $\pm$ 0.0008) compared with PHz-intoxicated mice ($p < 0.0001$, one-way ANOVA) and close to control mice (Figure 4D).

H&E-stained spleen sections of the control and Mn-citrate-NC-treated groups showed normal histological features, which comprised of ideal red and white pulp region (Figures 4E and S5). The spleen sections from PHz-administered mice displayed severe pathological damages such as white pulp atrophy and red pulp degeneration (Figures 4E and S5). Treatment with Mn-citrate NC notably reduced splenic tissue necrosis (Figure 4 e and f). It also showed normal white pulp region and increasing red pulp area with extramedullary hematopoietic cells. It indicates increased erythropoiesis in spleen under hypoxia due to increased erythropoietin production (Bozzini et al., 1970). Overall, Mn-citrate NC was able to efficiently impede the marked detrimental changes in the spleen architecture of anemic animals.

The nano-complex ameliorates inflammatory response

As reported, immune activation, especially elevation in the lymphocyte population, is closely associated with PHz-induced anemia (Naughton et al., 1990), and our study also found high level of white blood cell count in CBC parameter and blood smear, we analyzed splenic T-lymphocyte subgroups ($CD4^+$ and $CD8^+$ cells) by flow cytometry to know the overall inflammation status of the system in anemia of inflammation mice model (Mcbride and Striker, 2017). As shown in Figure 5A, there was remarkable decrease in the ratio of splenic $CD4^+/CD8^+$ T-lymphocytes of PHz-treated mice ($CD4^+/CD8^+$ T-lymphocytes: 1.56 $\pm$ 0.06; $p < 0.0001$; $F(3, 32.43) = 67.72$, one-way ANOVA) in comparison to control mice ($CD4^+/CD8^+$ T-lymphocytes: 2.02 $\pm$ 0.08). Mice co-treated with PHz + Mn-citrate NC showed notably higher ratio of $CD4^+/CD8^+$ T-lymphocytes ($CD4^+/CD8^+$ T-lymphocytes: 2.01 $\pm$ 0.10) than PHz-intoxicated mice ($p < 0.0001$). No difference was observed between the Mn-citrate-NC-treated and the control groups ($p = 0.0848$). The histopathological examination of spleen tissues of PHz-intoxicated mice also indicated toward the same phenomenon i.e. infiltration of inflammatory cells i.e. macrophages. And it also demonstrated the reduction in inflammatory cells population in PHz + Mn-citrate NC co-treated mice than PHz-treated mice (Figure 4E). So, we also performed touch preparation of spleen to evaluate the extent of tissue-resident macrophages i.e. histiocytes. Leishman's-stained spleen smear showed extremely high percentage of histiocytes in PHz-intoxicated mice. We observed a very low number of histiocytes in spleen of PHz + Mn-citrate NC co-treated mice (Figure 5G, right). So, these results indicated toward severe inflammatory response generated by PHz administration and functioning of Mn-citrate NC as preventive agent against inflammation in physiological milieu.

The molecular and histopathological examination findings propelled us to evaluate the pro-inflammatory cytokines levels in the physiological milieu. Macrophage and other lymphocytes infiltration generally followed by subsequent rise in tumor necrosis factor alpha (TNF-α), interferon gamma (IFN-γ), and other cytokines (Adhikari et al., 2021a, 2021b; Arango Duque and Descoteaux, 2014). So, we evaluated time-dependent expression of different cytokines in blood over the recovery period of our study (Figure S6). We found significant increases in plasma concentrations of TNF-α, IFN-γ, interleukin-6 (IL-6), IL-1β, and IL-10 in PHz-administered animals (Figure 5B–5F). Co-treatment with PHz + Mn-citrate NC successfully prevented the increase in the cytokine levels. Moreover, mice treated with PHz + Mn-citrate NC showed almost normal level of cytokines in blood on day 6 (Figure S6). In contrast, only PHz-treated mice showed remarkably high level of cytokines on day 6. No difference was observed between the Mn-citrate-NC-treated and the control groups. These results strongly indicate toward the anti-inflammatory potential of Mn-citrate NC in treatment of anemia of inflammation.

Several studies have also reported that inflammation (mainly cytokines)-induced hypoferremia is one of the clinical manifestations in anemia of inflammation. It is caused due to excessive iron sequestration in the

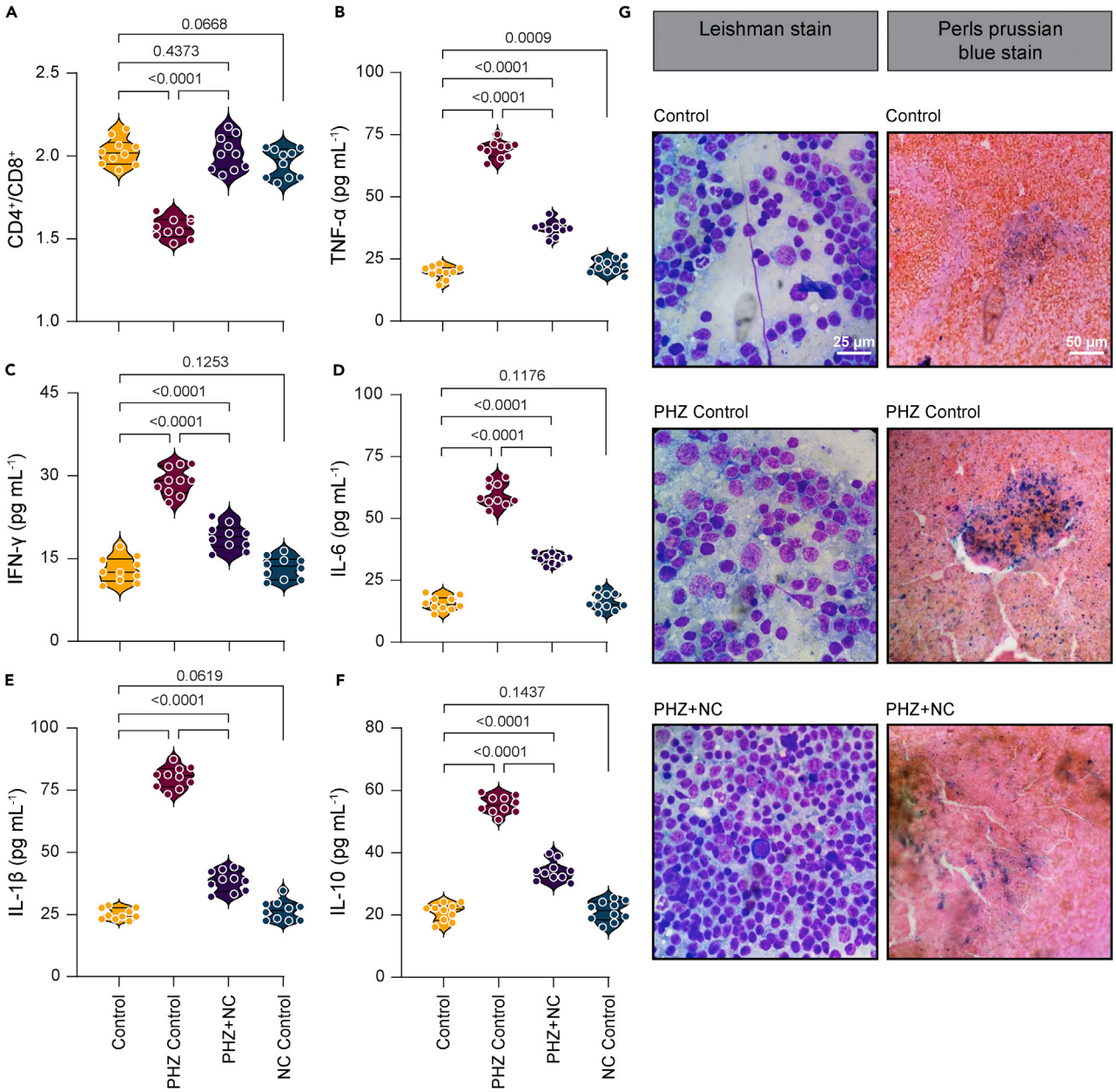

Figure 5. Role of Mn-citrate nanocomplex in amelioration of inflammatory response

(A) $CD4^+/CD8^+$ T-lymphocytes ratio. (B) Serum TNF-α level. (C) Serum IFN-γ level. (D) Serum IL-6 level. (E) Serum IL-1β level. (F) Serum IL-10 level. (G) Touch preparation of spleen tissue stained with Leishman stain; scale bar: 25 μm (Right) and Perls' Prussian blue stain (Left); scale bar: 50 μm. Data are expressed as mean ± SD (n = 10). Individual data points are represented as colored circles (n = 10). One-way ANOVA followed by correction of false discovery rate (post hoc FDR: two-stage step up method of Benjamini, Krieger, and Yekutieli) for multiple comparisons was performed for comparison between multiple groups. See also Figure S6.

macrophages of reticuloendothelial system, which comprises liver, spleen, and lung (Ganz and Nemeth, 2009; Weiss and Goodnough, 2005). So, we prepared touch preparations of spleen for iron stain. Perls' Prussian-blue-stained spleen touch preparation of PHz-administered mice showed very high level of iron storage in comparison to control mice (Figure 5G, left). On the other hand, co-treatment with PHz + Mn-citrate NC resulted in a remarkable decrease in the iron storage level in spleen (Figure 5G, left). These results clearly indicated that the treatment with Mn-citrate NC prevents inflammation-mediated excessive iron sequestration in spleen.

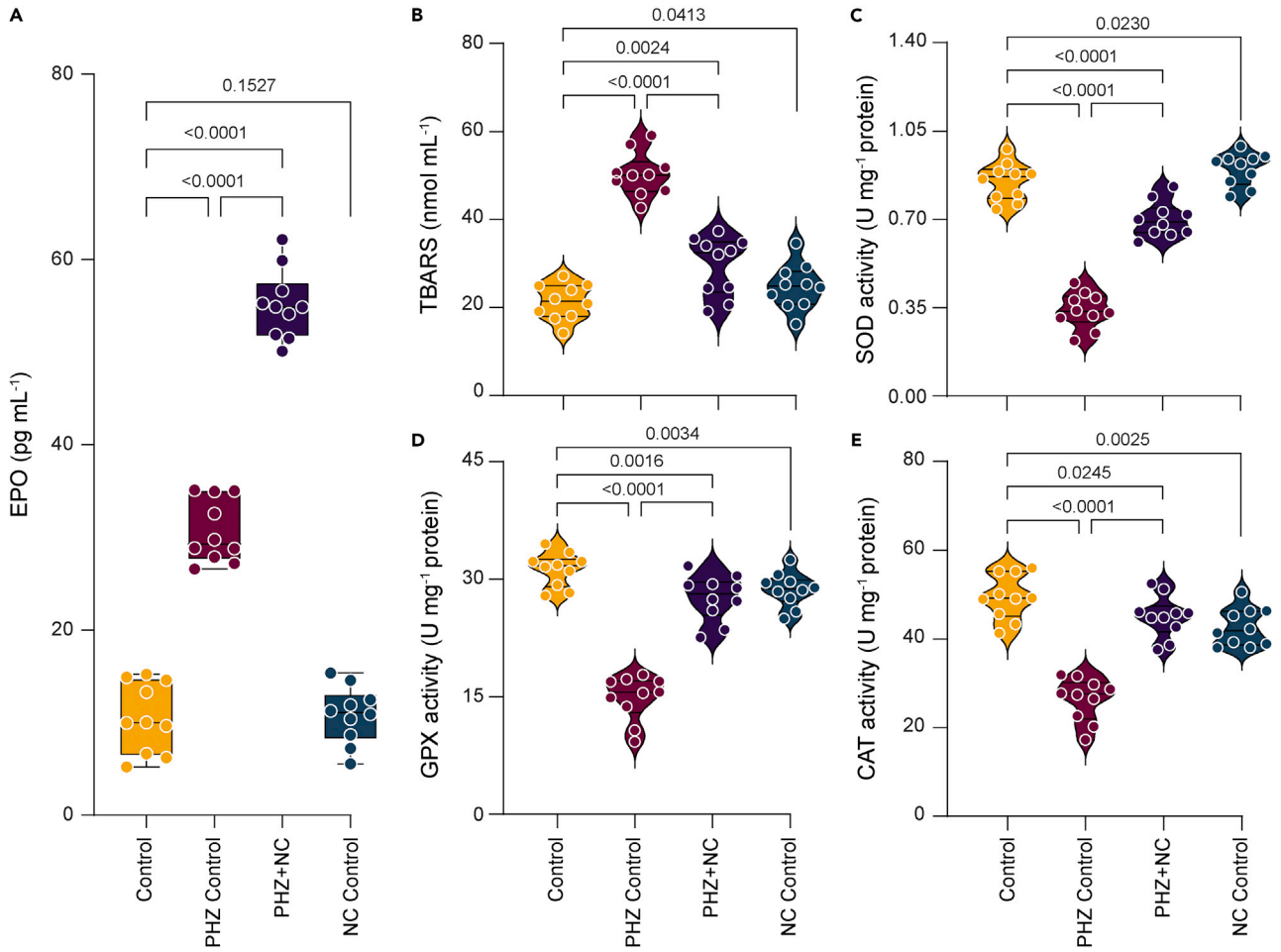

Figure 6. Ability of Mn-citrate nanocomplex to act as an erythropoiesis-stimulating agent in protection of RBCs from oxidative damage

(A) Erythropoietin (EPO) concentrations. (B) Extent of lipid peroxidation (MDA, malonaldehyde content) measured in terms of thiobarbituric acid reactive substances (TBARS).

(C) Superoxide dismutase (SOD) activity.

(D) Gluthione peroxidase (GPx) activity.

(E) Catalase (CAT) activity. Data are expressed as mean ± SD (n = 10). Individual data points are represented as colored circles (n = 10). One-way ANOVA followed by correction of false discovery rate (post hoc FDR: two-stage step up method of Benjamini, Krieger, and Yekutieli) for multiple comparisons was performed for comparison between multiple groups. See also Figures S7 and S2.

The nano-complex reduces oxidative damage associated with anemia of inflammation

The progression of anemia is closely associated with the oxidative status of the system. Therefore, we have evaluated the extent of lipid peroxidation, a potential biomarker for oxidative damage to test the efficacy of Mn-citrate NC on protection against oxidative-stress-induced damages (Niki, 2008). The malondialdehyde (MDA)level was over 2-fold higher in PHz-treated mice (MDA: 50.26 ± 4.95 nmol MDA ml^{-1}; $p < 0.0001$, $F (5, 49.42) = 39.36$, one-way ANOVA) compared with control group (MDA: 21.32 ± 4.08 nmol MDA ml^{-1}) (Figure 6B). These findings confirmed that the oxidative damage had been successfully induced by PHz administration. At the same time co-treated mice showed remarkably less MDA content (MDA: 29.56 ± 6.67 nmol MDA ml^{-1}) compared with PHz-administered group ($p < 0.0001$, one-way ANOVA); this suggests that the Mn-citrate NC played a significant role in diminishing the oxidative damage. We also monitored the level of different antioxidant enzymes in RBCs to investigate the supportive role of Mn-citrate NC against oxidative stress in the physiological milieu on day 4. There was a significant decline in SOD (~60%), CAT (~41.04%), and GPx (~52.51%) activities in PHz-treated mice compared with control group (SOD: $p < 0.0001$, $F (5, 52.53) = 97.07$, one-way ANOVA; CAT: $p < 0.0001$, $F (5, 52.78) = 32.33$, one-way ANOVA; GPx: $p < 0.0001$, $F (5, 51.10) = 58.85$, one-way ANOVA). Co-treated mice demonstrated

remarkably higher SOD (~105.88%), CAT (~54.46%), and GPx (~86.24%) activities compared with PHz-intoxicated mice ($p < 0.0001$, one-way ANOVA) (Figures 6C–6E). Thus, treatment with Mn-citrate NC showed excellent efficacy in strengthening the antioxidant defense system of RBCs to combat oxidative stress.

The nano-complex upregulates erythropoietin synthesis

Previous studies illustrated the potential role of ROS (cellular oxidative status) in EPO production and consequent erythropoiesis including hypoxia-induced erythropoiesis (Fandrey et al., 1994, 1997; Zhao et al., 2016). As our results suggest that the Mn-citrate NC has cellular redox modulatory properties, we measured time-dependent expression of the serum EPO level over the recovery period of our study to assess the effect of Mn-citrate NC on EPO synthesis (Figure S7).

Surprisingly, in our phase-1 study, co-treated mice demonstrated a 1.79-fold higher EPO level (EPO: 55.12 ± 3.72 pg ml^{-1}; $p < 0.0001$, $F(3, 35.11) = 362.2$, one-way ANOVA) compared with PHz-treated mice (EPO: 30.66 ± 3.42 pg ml^{-1}) on day 4. In fact, co-treated mice had around 5-fold higher EPO level compared with control mice (EPO: 10.56 ± 3.77 pg ml^{-1}, $p < 0.0001$, one-way ANOVA) (Figure 6A). Further investigation showed that single oral dose of Mn-citrate NC maintained around 2.68-fold higher EPO level (EPO: 32.07 ± 3.89 pg ml^{-1}; $p < 0.0001$, $F(3, 32.20) = 106.5$, one-way ANOVA) compared with control mice (EPO: 11.96 ± 3.03 pg ml^{-1}) on day 8 (Figure S7).

Again, in our phase-2 study, we found a 2.32-fold higher EPO level in mice treated with Mn-citrate NC (EPO: 93.29 ± 4.56 pg ml^{-1}; $p < 0.0001$, $F(3, 31.56) = 1131$, one-way ANOVA) compared with PHz-administered mice (EPO: 40.09 ± 3.47 pg ml^{-1}) on day 5. Most surprisingly, Mn-citrate NC-treated mice showed ~9-fold higher EPO level in comparison to control mice (EPO: 10.56 ± 3.77 pg ml^{-1}; $p < 0.0001$, one-way ANOVA) (Figure 3E). So, these results support the observed high level of erythropoiesis (i.e., production of RBCs) induced with single oral dose of Mn-citrate NC via stimulation of EPO production in anemic mice. As kidney plays a vital role in erythropoiesis, we have analyzed the structural integrity of hematoxylin and eosin (H&E)-stained kidney sections under microscope to assess whether treatment with Mn-citrate NC caused any kind of damage to kidney or not. The histological analysis of kidney showed no damage, and the normal structure of medulla and cortex was maintained in Mn-citrate-NC-treated mice (Data not shown here). So, treatment with Mn-citrate NC did not cause any kind of toxicity to kidney in mice.

The reason behind upregulated erythropoietin synthesis

One of the main physiological reasons behind the upregulation of EPO synthesis may be induction of local hypoxia and modulation of hypoxia-induced EPO synthesis (HIF system) pathway. Previous studies have shown that some transition metals (cobalt, nickel, and manganese) can mimic the hypoxic state by substituting the ferrous iron of the newly synthesized porphyrin ring, thereby locking the heme protein in the deoxy conformation just as at low oxygen tension and resulting in stimulation of EPO production (Goldberg et al., 1988; Huang et al., 1997). To test this hypothesis, we tested whether Mn-citrate NCs can successfully be incorporated into the newly synthesized protoporphyrin ring of hemoglobin. We studied the interaction of Mn-citrate NC with the porphyrin rings of hematoporphyrin (hp) using steady state fluorescence spectroscopy.

In the photoluminescence study, hematoporphyrin showed a strong emission at ~616 nm and another emission peak of lower intensity at ~677 nm, on excitation at ~410 nm (Figure S2A). In the presence of Mn-citrate NC, the fluorescence intensities of both the emission peaks reduced drastically due to the incorporation of the NC in the porphyrin moiety (Patwari et al., 2018). This phenomenon of fluorescence quenching can be due to various molecular events e.g. molecular re-arrangements, ground-state complex formation, energy transfer, and excited state collisional quenching. In this case, no discernable shift in the emission maxima or shape in the fluorescence spectra was observed, instead the quenching behavior adhered to the Stern-Volmer equation.

The upward curvature of the Stern-Volmer plot (Figure S2A, inset) without any dependence on the NC signifies that neither simple nor dynamic (linear F_0/F vs [Mn-citrate NC] nor combined static or dynamic (second-degree polynomial) quenching model was able to describe the quenching model. Thus, a combined "sphere of action" dynamic quenching model was required to describe the quenching behavior of hematoporphyrin with Mn-citrate NC. This signifies that by means of Poisson distribution, the probability of an NC is significant enough to quench the fluorophore hematoporphyrin. The deviation from the linear

Stern-Volmer behavior can be due to the plausible Coulombic interactions between hematoporphyrin and Mn-citrate NC in the excited state. This could be further supported by the time-resolved studies that show a decrease in lifetime of the fluorophore. The functional form of the quenching model is

$$\frac{F_0}{F} = (1 + K_D[Q])e^{(K_e[Q])}$$

where F_0 and F are the fluorescence intensities in the absence and presence of the quencher molecule [Q], which is the Mn-citrate NC; K_D and K_e are the Stern-Volmer quenching constant. The constants K_D and K_e were found by nonlinear least-squares regression of the data.

The value of bimolecular quenching constant $k_q(K_D/\tau_0)$ has been found to be $\sim 6.71 \times 10^{12}\ M^{-1}s^{-1}$, which is more than the diffusion control limit ($\sim 10^{10}\ M^{-1}s^{-1}$). This in turn indicates binding of the Mn-citrate NC with hematoporphyrin. The double logarithmic plot reveals an association constant of $6.3 \times 10^3\ M^{-1}$ and the number of binding sites (n) to be 0.7, according to the equation

$$\log\frac{F_0 - F}{F} = \log K_a + n\log[Q]$$

where K_a denotes the association constant and n indicates the number of binding sites. This indicates a molecular binding between hematoporphyrin and Mn-citrate NC ions forming a stable complex with a mole ratio of ~0.7:1 in between hematoporphyrin and Mn-citrate NC (Patwari et al., 2018). Thus, spectroscopic studies confirm a strong binding of Mn-citrate NC with the porphyrin moiety of hematoporphyrin molecule (Figure S2B–S2D).

DISCUSSION

In this study, we report synthesis, characterization, and unique *in vivo* prophylactic as well as therapeutic activity of an erythropoiesis-stimulating nano-agent (nano-ESA), Mn-citrate nanocomplex (~2–5 nm diameter) against anemia, particularly anemia of inflammation. We provide direct evidence that orally administrable nano-ESA (0.25 mg kg^{-1} BW) can increase both Hb-level (Hb: 13.11 ± 0.48 g dL^{-1} compared with 8.07 ± 0.59 g dL^{-1} of the anemic model) and erythrocyte count (RBC: 6.21 ± 0.31 10^6 μL^{-1} compared with 3.98 ± 0.35 10^6 μL^{-1} of the anemic model) in the systemic circulation of the chemical-induced rodent model of severe anemia. Treatment with nano-ESA also impedes extent of hemolysis, maintains structural integrity as well as increases osmotic resistance capacity of erythrocytes. The histopathological and molecular analysis of the spleen indicates significant decline in inflammatory markers like cytokines, helper T cells ($CD4^+$cells), cytotoxic T cells ($CD8^+$cells), macrophages etc. The molecular mechanism of action of this nano-ESA is multifaceted (Figure 7): (1) amelioration of inflammatory response; (2) reduction of the oxidative distress, a causal factor for the destruction of RBC in several disease conditions; and (3) upregulation of EPO synthesis through binding to free porphyrins, in turn, simulating a condition of hypoxia.

PHz intoxication has long been considered a classic model to study effectiveness of new drug molecules against anemia, as it closely resembles the pathophysiological conditions in humans (Hara and Ogawa, 1976; Itano et al., 1975; Lee et al., 2014). Apart from oxidative destruction of erythrocyte membrane proteins, PHz stimulates production of autologous immunoglobulin G (IgG), which on being recognized by macrophage Fc receptor mechanism triggers rapid erythrophagocytosis in the spleen and liver (Naughton et al., 1990). Furthermore, several studies have indicated that free heme and hemoglobin released by rapid erythrocyte breakdown (hemolysis) subsequently induce high level of oxidative distress resulting in inflammatory response and excessive cytokine production leading to the pathophysiological condition of anemia of inflammation (Sparkenbaugh et al., 2015; Wagener et al., 2001; Schaer et al., 2013; Bozza and Jeney, 2020). In this context, treatment with Mn-citrate NC already showed excellent efficacy in strengthening the antioxidant defense system of RBCs to combat oxidative stress and associated damages. So, nano-ESA is functioning as a redox-modulating agent to maintain redox homeostasis in the physiological milieu. As a result, nano-ESA can reduce the systemic inflammatory response through maintaining normal oxidative status of the system. And nano-ESA also prevents hemolysis through reduction of oxidative distress, which leads to reduced hemolysis. In continuation to our discussion, we have observed severely low ratio of splenic $CD4^+/CD8^+$ T-lymphocytes [0.5] in PHz-intoxicated anemic mice, indicating altered immune activity, immune senescence, and especially a state of chronic inflammation (Mcbride and Striker, 2017; Appay and Sauce, 2008; Wikby et al., 2005). Interestingly treatment with nano-ESA significantly improved the $CD4^+/CD8^+$ ratio [1.4]. Further, our results clearly demonstrate that treatment with nano-ESA downregulates

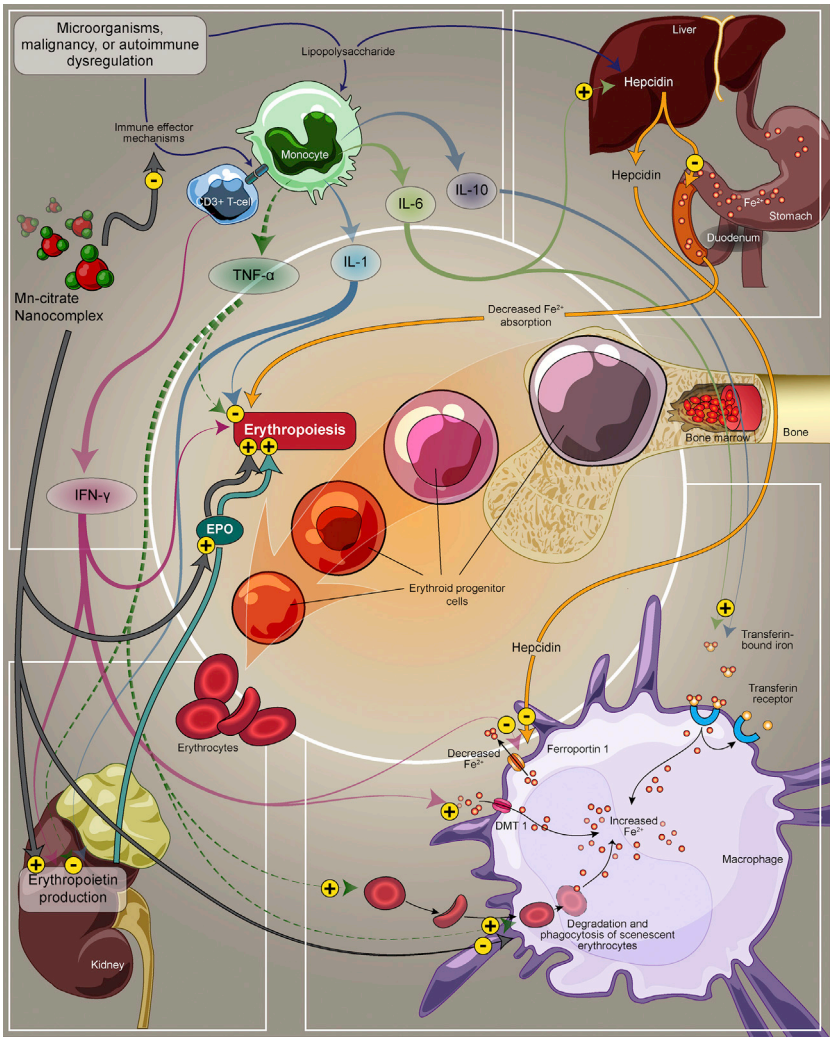

Figure 7. Pathophysiological mechanism of action of Mn-citrate nanocomplex in treatment of anemia of inflammation

The microbial invasion, appearance of malignant cells, or immune dysregulation causes hyperactivation of T cells and monocytes in physiological milieu. These cells elicit different immune effector pathways like production of cytokines from T cells (IFN-γ) and monocytes or macrophages (TNF-α, IL-6, IL-1β, and IL-10). And those cytokines' activities lead to a diminished the free iron level in circulation by different ways and thus to a reduced availability of iron for erythropoiesis and development of anemia. Mn-citrate nanocomplex prevents anemia of inflammation condition by (A) inhibiting the immune effector mechanisms, (B) upregulation of erythropoietin (EPO) synthesis through binding to free porphyrins, in turn stimulating a condition of hypoxia, and (C) preventing the destruction of RBCs through reducing oxidative stress in physiological milieu. Plus signs represent stimulation and minus signs represent inhibition. DMT1; divalent metal transporter 1.

the pro-inflammatory markers like TNF-α, IFN-γ, and other cytokines (IL-6, IL-1β, and IL-10), which have previously been described as the causative cytokines produced by the inflammatory cells particularly in severe state of anemia of inflammation.

A hallmark of this kind of anemia is the pro-inflammatory-cytokines-induced dysregulation of iron homeostasis in physiological milieu, with increased uptake and retention of iron within the cells of reticuloendothelial system (RES) like liver, spleen, lung etc (Weiss and Goodnough, 2005) (Ganz and Nemeth, 2009). It leads to a shifting of iron pool from the circulation into the storage sites of the RES. And this diversion causes limitation of the availability of iron for erythroid progenitor cells, which leads to iron-restricted erythropoiesis in physiological milieu. In addition to that, the acquisition of iron predominantly takes place

through erythrophagocytosis by macrophages in anemia of inflammation. Our results also showed high level of iron storage and macrophages in spleen tissue of PHz-intoxicated anemic mice. In this context, we found treatment with nano-ESA remarkably reduces the excessive iron sequestration in tissues and also decreases macrophages, which help to maintain iron homeostasis in the physiological system. Therefore, amelioration of inflammatory response is probably one of the several mechanisms that contribute to the therapeutic activity of the nano-ESA. The reduction of splenomegaly and restoration of normal spleen architecture as observed in the histopathological analysis further supports this argument.

We have used citrate in preparation of nano-ESA (Mn-citrate nanocomplex) to make the nanocomplex stable and soluble in water at physiological environment. Previous publications showed that isocitrate can be used in treatment of anemia of inflammation through inducing reticulocytosis, suppressing erythroid iron restriction response etc. These studies also indicate a very high amount of isocitrate required for effective response and also lacks EPO enhancing property (Richardson et al., 2013) (Kim et al., 2016). But in our study, we did not observe any kind of significant beneficial role of citrate in treatment of anemia of inflammation. It may be due to the very low amount of citrate (0.15 mg kg^{-1} BW) used in our study as this very low amount of citrate is required for the preparation of therapeutic dose of Mn-citrate NC.

Oxidative damages and inflammation are known to be tied together in the physiological systems (Hajjar and Gotto, 2013; Mittal et al., 2014; Forrester et al., 2018). PHz creates significant oxidative damage to the erythrocyte membranes as indicated by high lipid peroxidation content in the blood of the PHz-treated animals. The level of lipid peroxidation was significantly lowered and an enhancement in the activity of the antioxidant enzymes (e.g., SOD, CAT, GPx) was observed in mice co-treated with PHz and nano-ESA. It is worth mentioning here that the SOD, CAT, and GPx triad forms the basis of fundamental of cellular response to oxidative damage (Adhikari et al., 2018). Therefore, together the results are suggestive of the protective activity of nano-ESA from oxidants that plays a crucial role in decreasing the pro-inflammatory activity, in turn, preventing the RBCs from destruction.

Acute anemic stress induces tissue hypoxia, which leads to the activation of a physiological stress response called stress erythropoiesis designed to improve oxygen delivery to tissues. The increased erythropoiesis is a key component of this response. Previous studies suggested that as anemia progresses, tissue hypoxia increases and leads to the induction of erythropoietin expression in the kidney. The increase in serum EPO concentration drives the expansion and differentiation of bone marrow erythroid progenitors. In the mouse, stress erythropoiesis predominantly occurs in the spleen (Paulson et al., 2011) (Wang et al., 2021). In this study, we have observed severe pathological damages like white pulp atrophy, red pulp degeneration, and no trace of extramedullary hematopoietic cells in spleen due to PHz intoxication. And PHz-intoxicated mice also showed insufficient amount of EPO in blood. So, these results indicate that erythropoiesis pathway is not functioning well due to oxidative damage and other detrimental effects of PHz intoxication. Interestingly, treatment with nano-ESA notably reduced splenic tissue necrosis and increased normal white pulp region and red pulp area with extramedullary hematopoietic cells. It indicates increased erythropoiesis in spleen due to increased erythropoietin production. And we have also found elevated EPO level in nano-ESA-treated mice. Further, we did not find any kind of detrimental effect in kidney of nano-ESA treated mice. So, another possible mechanism behind the therapeutic action could be the induction of EPO synthesis by nano-ESA administration. EPO and its long-acting analogs are widely used to support erythropoiesis in patients with CKD, cancer, and other forms of anemia associated with insufficient endogenous production of it (Macdougall, 2012). Theoretically, alternative approaches that stimulate EpoR may have additional clinical benefits when compared with EPO-based therapies, including oral bioavailability and/or additional erythropoietic activities (Wrighton et al., 1996). Here, the observed upregulation of EPO synthesis may have occurred via the hypoxia-inducible factor (HIF)-1-related signaling pathway. HIF-1 is a heterodimeric transcription factor stabilized in hypoxic conditions. Stabilized HIF-1 translocates to the nucleus to bind to hypoxia response elements in a cassette of genes that mediate adaptive responses to combat hypoxia. HIF-1 consists of an oxygen-regulated α-subunit (*HIF*-1α) and a constitutively expressed β-subunit (*HIF*-1β). *HIF*-1α is rapidly degraded under normoxic conditions by the ubiquitin-proteosome system. Hypoxic condition upregulates *HIF*-1α, thereby allowing it to accumulate in high levels and dimerize with *HIF*-1β. HIF-mediated adaptive responses to hypoxia induce coordinated erythropoiesis through upregulation of EPO synthesis in liver and kidney, activation of EPO receptor, and downregulation of hepcidin, an erythropoiesis inhibitory molecule secreted from liver (Locatelli et al., 2017). Our spectroscopic studies further enlighten this mechanism; the results indicate successful incorporation of nano-ESA

into the protoporphyrin ring of hemoglobin, in the physiological milieu. The nano-ESA-substituted hemoglobin (in a regulated manner) is locked in the deoxy conformation similar to low oxygen tension mimicking the state of local hypoxia, thereby activating the HIF-mediated adaptive response. As a result, EPO synthesis gets upregulated. In addition, nano-ESA may have another route of action, i.e. inhibition of the prolyl hydroxylase (PHD) enzymes, which regulates the stabilization of the HIF according to the oxygen availability in physiological milieu. During low oxygen availability, the inhibition of PHD allows the stabilization of HIF for the cellular adaptation to hypoxia (Nguyen and Duran, 2016). In addition to that the PHD enzyme contains Fe^{2+} in their catalytic centers. Previous studies showed that many metal ions such as manganese, zinc, nickel, and cobalt are widely used hypoxia mimic and work by substituting iron in the active center of HIF PHD to inactivate the enzyme and to stabilize HIF. Furthermore, a more detailed molecular study including erythrocyte turnover and reticulocytosis could clarify the exact mechanism of action. However, the prophylactic as well as therapeutic efficiency of the nano-ESA is very promising and may serve as the cornerstone in translating this study to the clinical trials.

Limitations of the study

One major limitation of this study is the use of chemical-induced model of anemia. Although, widely accepted, the PHz model could be replaced by more robust knockout animal models, which eventually could provide more insight into the mechanism. A detailed toxicity study along with information on pharmacokinetics and pharmacodynamics of the nano-ESA would pave its way to the clinical trials. Furthermore, molecular experiments are required to solve the exact mechanism of action of nano-ESA in the light of expression of *HIF*-1α in physiological milieu.

Conclusion

In conclusion, our results suggest that the synthesized Mn-citrate nanocomplex possess potential erythropoiesis stimulatory (through upregulation of EPO) as well as anti-inflammatory properties, which in turn have played significant role in the treatment of anemia of inflammation in experimental animal model. The mechanism behind such unprecedented therapeutic activity may open a new array of treatment strategies against numerous diseases associated with oxidative stress, redox imbalance, autoimmune condition, and hypoxia in near future. In addition, comprehensive molecular study analyzing the genome and metabolome of Mn-citrate-NC-treated animals may illuminate its ability to interfere in other important metabolic or pathophysiological pathways. Although found biocompatible in our study, a detailed subchronic toxicity study is important for successful clinical translation of this nanocomplex. Nevertheless, the nano-complex has the potential to become a medical weapon of rapid recovery in the fight against anemia of inflammation.

STAR★METHODS

Detailed methods are provided in the online version of this paper and include the following:

- KEY RESOURCES TABLE
- RESOURCE AVAILABILITY
  - Lead contact
  - Materials availability
  - Data and code availability
- EXPERIMENTAL MODEL AND SUBJECT DETAILS
  - Rodent model
- METHOD DETAILS
  - Materials
  - Synthesis of Mn-citrate NC
  - Characterization techniques
  - Study design
  - Phase 1
  - Phase 2
  - Dosing description
  - Induction of anemia
  - Measurement of hemoglobin concentration
  - Blood collection
  - Assessment of hematological parameters

- Blood film preparation and staining
- Evaluation of osmotic resistance of RBCs
- Histopathological examination
- Cell preparation and flow cytometry analysis
- RBC hemolysate preparation
- Assessment of lipid peroxidation and antioxidant enzyme activity
- Serum isolation
- Measurement of erythropoietin and inflammatory cytokines level
- Evaluation of interaction of Mn-citrate NC with the porphyrin rings of hematoporphyrin

● QUANTIFICATION AND STATISTICAL ANALYSIS

SUPPLEMENTAL INFORMATION

Supplemental information can be found online at https://doi.org/10.1016/j.isci.2022.105021.

ACKNOWLEDGMENTS

The authors thank Paw Path Diagnostic Laboratory for Animals, Kolkata, West Bengal for performing hematology tests. We also thank the animal caretakers of Central Animal Facility, Dept. of Zoology, Uluberia College, Howrah, West Bengal. The authors would like to acknowledge the CRNN, University of Calcutta, Kolkata, West Bengal. MD thanks University Grants Commission (UGC), Govt. of India for Junior Research Fellowship grant (UGC Ref. No.: 651/(CSIR-UGC NET JUNE 2019). This study was supported by Indian National Academy of Engineering (INAE) for the Abdul Kalam Technology Innovation National Fellowship (INAE/121/AKF) and DBT (WB)-BOOST scheme for the financial grant (339/WBBDC/1P-2/2013). The authors would like to acknowledge the Deanship of Scientific Research at Umm Al-Qura University, for supporting this work by Grant code: 22UQU4320545DSR20. Dr. Ziad Moussa is grateful to the United Arab Emirates University(UAEU) of Al-Ain and to the Research Office for supporting the research developed in his laboratory (Grant no. G00003291).

AUTHOR CONTRIBUTIONS

Conceptualization: M.D., S.M., A.A., J.K.K., and S.K.P. Methodology: M.D., S.M., R.G., P.B., A.A., S.D., and Z.M. Investigation: M.D., S.M., R.G., and A.K.D. Visualization: M.D., S.M., and A.A. Funding Acquisition: S.K.P., D.P., S.A.A., and Z.M. Project Administration: S.K.P., J.K.K., and S.S.B. Supervision: S.K.P., D.P., S.S.B., J.K.K., A.K.M., A.K.D., P.C., and S.A.A. Writing—Original Draft: M.D., S.M., R.G., and P.B. Writing—Review and Editing: S.K.P., A.A., J.K.K., P.C., and S.D.

DECLARATION OF INTERESTS

S.K.P., A.K.M., A.A., and P.C. have submitted a patent application (Reference Number: 202131034977) related to Mn-citrate NC and its efficacy in treatment of anemia. All other authors declare that they have no competing interests.

Received: May 2, 2022
Revised: June 20, 2022
Accepted: August 19, 2022
Published: September 16, 2022

REFERENCES

Aapro, M.S., and Link, H. (2008). September 2007 update on EORTC guidelines and anemia management with erythropoiesis-stimulating agents. Oncol. *13*, 33–36. https://doi.org/10.1634/theoncologist.13-S3-33.

Adamson, J.W. (2008). The anemia of inflammation/malignancy: mechanisms and management. Hematology Am. Soc. Hematol. Educ. Program. 159–165. https://doi.org/10.1182/asheducation-2008.1.159.

Adhikari, A., Darbar, S., Chatterjee, T., Das, M., Polley, N., Bhattacharyya, M., Bhattacharya, S., Pal, D., and Pal, S.K. (2018). Spectroscopic studies on dual role of natural flavonoids in detoxification of lead poisoning: bench-to-bedside preclinical trial. ACS Omega *3*, 15975–15987. https://doi.org/10.1021/acsomega.8b02046.

Adhikari, A., Mondal, S., Chatterjee, T., Das, M., Biswas, P., Ghosh, R., Darbar, S., Alessa, H., Althakafy, J.T., Sayqal, A., et al. (2021a). Redox nanomedicine ameliorates chronic kidney disease (CKD) by mitochondrial reconditioning in mice. Commu. Biol. *4*, 1013. https://doi.org/10.1038/s42003-021-02546-8.

Adhikari, A., Mondal, S., Das, M., Biswas, P., Pal, U., Darbar, S., Bhattacharya, S.S., Pal, D., Sahadasgupta, T., Das, A.K., et al. (2021b). Incorporation of a biocompatible nanozyme in cellular antioxidant enzyme cascade reverses huntington's like disorder in preclinical model. Adv. Healthc. Mater. *10*, e2001736. https://doi.org/10.1002/adhm.202001736.

Adhikari, A., Polley, N., Darbar, S., Bagchi, D., and Pal, S.K. (2016). Citrate functionalized Mn3O4 in nanotherapy of hepatic fibrosis by oral administration. Future Sci. OA. *2*, FSO146. https://doi.org/10.4155/fsoa-2016-0029.

Anselmo, A.C., and Mitragotri, S. (2016). Nanoparticles in the clinic. Bioeng. Transl. Med. *1*, 10–29. https://doi.org/10.1002/btm2.10003.

Appay, V., and Sauce, D. (2008). Immune activation and inflammation in HIV-1 infection: causes and consequences. J. Pathol. *214*, 231–241. https://doi.org/10.1002/path.2276.

Arango Duque, G., and Descoteaux, A. (2014). Macrophage cytokines: involvement in immunity and infectious diseases. Front. Immunol. *5*, 491. https://doi.org/10.3389/fimmu.2014.00491.

Benjamini, Y., Krieger, A.M., and Yekutieli, D. (2006). Adaptive linear step-up procedures that control the false discovery rate. Biometrika *93*, 491–507. https://doi.org/10.1093/biomet/93.3.491.

Bennett-Guerrero, E., Veldman, T.H., Doctor, A., Telen, M.J., Ortel, T.L., Reid, T.S., Mulherin, M.A., Zhu, H., Buck, R.D., Califf, R.M., and Mcmahon, T.J. (2007). Evolution of adverse changes in stored RBCs. Proc. Natl. Acad. Sci. USA *104*, 17063–17068. https://doi.org/10.1073/pnas.070816010.

Bobo, D., Robinson, K.J., Islam, J., Thurecht, K.J., and Corrie, S.R. (2016). Nanoparticle-based medicines: a review of FDA-approved materials and clinical trials to date. Pharm. Res. (N. Y.) *33*, 2373–2387. https://doi.org/10.1007/s11095-016-1958-5.

Boutou, A.K., Hopkinson, N.S., and Polkey, M.I. (2015). Anaemia in chronic obstructive pulmonary disease: an insight into its prevalence and pathophysiology. Clin. Sci. (Lond.). *128*, 283–295. https://doi.org/10.1042/CS20140344.

Bozza, M.T., and Jeney, V. (2020). Pro-inflammatory actions of heme and other hemoglobin-derived DAMPs. Front. Immunol. *11*, 1323. https://doi.org/10.3389/fimmu.2020.01323.

Bozzini, C.E., Barrio Rendo, M.E., Devoto, F.C., and Epper, C.E. (1970). Studies on medullary and extramedullary erythropoiesis in the adult mouse. Am. J. Physiol. *219*, 724–728. https://doi.org/10.1152/ajplegacy.1970.219.3.724.

Brittenham, G.M., Klein, H.G., Kushner, J.P., and Ajioka, R.S. (2001). Preserving the national blood supply. Hematology Am. Soc. Hematol. Educ. Program. *422–32*. https://doi.org/10.1182/asheducation-2001.1.422.

Camaschella, C. (2015). Iron-deficiency anemia. N. Engl. J. Med. *372*, 1832–1843. https://doi.org/10.1056/NEJMra1401038.

Camaschella, C. (2019). Iron deficiency. Blood *133*, 30–39. https://doi.org/10.1182/blood-2018-05-815944.

Chatterjee, T., De, D., Chowdhury, S., and Bhattacharyya, M. (2020). Nuclear factor NF-kappaB1 functional promoter polymorphism and its expression conferring the risk of Type 2 diabetes-associated dyslipidemia. Mamm. Genome *31*, 252–262. https://doi.org/10.1007/s00335-020-09846-0.

Chatterjee, T., Pattanayak, R., Ukil, A., Chowdhury, S., and Bhattacharyya, M. (2019). Autophagy protects peripheral blood mononuclear cells against inflammation, oxidative and nitrosative stress in diabetic dyslipidemia. Free Radic. Biol. Med. *143*, 309–323. https://doi.org/10.1016/j.freeradbiomed.2019.07.034.

Chmielewski, P.P., and Strzelec, B. (2018). Elevated leukocyte count as a harbinger of systemic inflammation, disease progression, and poor prognosis: a review. Folia Morphol. (Warsz). *77*, 171–178. https://doi.org/10.5603/FM.a2017.0101.

Churchill, D.N., Macarios, D., Attard, C., Kallich, J., and Goeree, R. (2007). Costs associated with erythropoiesis-stimulating agent administration to hemodialysis patients. Nephron Clin. Pract. *106*, c193–c198. https://doi.org/10.1159/000104431.

De Marchi, S., Pirisi, M., and Ferraccioli, G.F. (1993). Erythropoietin and the anemia of chronic diseases. Clin. Exp. Rheumatol. *11*, 429–444.

Ding, B., Yue, J., Zheng, P., Ma, P., and Lin, J. (2021). Manganese oxide nanomaterials boost cancer immunotherapy. J. Mater. Chem. B. *9*, 7117–7131. https://doi.org/10.1039/D1TB01001H.

Docherty, A.B., Turgeon, A.F., and Walsh, T.S. (2018). Best practice in critical care: anaemia in acute and critical illness. Transfus. Med. *28*, 181–189. https://doi.org/10.1111/tme.12505.

Erslev, A.J., and Besarab, A. (1997). Erythropoietin in the pathogenesis and treatment of the anemia of chronic renal failure. Kidney *51*, 622–630. https://doi.org/10.1038/ki.1997.91.

Fandrey, J., Frede, S., Ehleben, W., Porwol, T., Acker, H., and Jelkmann, W. (1997). Cobalt chloride and desferrioxamine antagonize the inhibition of erythropoietin production by reactive oxygen species. Kidney Int. *51*, 492–496. https://doi.org/10.1038/ki.1997.68.

Fandrey, J., Frede, S., and Jelkmann, W. (1994). Role of hydrogen peroxide in hypoxia-induced erythropoietin production. Biochem. J. *303* (Pt 2), 507–510. https://doi.org/10.1042/bj3030507.

Faquin, W.C., Schneider, T.J., and Goldberg, M.A. (1992). Effect of inflammatory cytokines on hypoxia-induced erythropoietin production. Blood *79*, 1987–1994.

Farrell, R.J., and Lamont, J.T. (1998). Rational approach to iron-deficiency anaemia in premenopausal women. Lancet *352*, 1953–1954. https://doi.org/10.1016/S0140-6736(05)61326-8.

Fischer, R., Simmerlein, R., Huber, R.M., Schiffl, H., and Lang, S.M. (2007). Lung disease severity, chronic inflammation, iron deficiency, and erythropoietin response in adults with cystic fibrosis. Pediatr. Pulmonol. *42*, 1193–1197. https://doi.org/10.1002/ppul.20717.

Forrester, S.J., Kikuchi, D.S., Hernandes, M.S., Xu, Q., and Griendling, K.K. (2018). Reactive oxygen species in metabolic and inflammatory signaling. Circ. Res. *122*, 877–902. https://doi.org/10.1161/CIRCRESAHA.117.311401.

Ganz, T. (2019). Anemia of inflammation. N. Engl. J. Med. *381*, 1148–1157. https://doi.org/10.1056/NEJMra1804281.

Ganz, T., and Nemeth, E. (2009). Iron sequestration and anemia of inflammation. Semin. Hematol. *46*, 387–393. https://doi.org/10.1053/j.seminhematol.2009.06.001.

Gil-Santana, L., Cruz, L.A.B., Arriaga, M.B., Miranda, P.F.C., Fukutani, K.F., Silveira-Mattos, P.S., Silva, E.C., Oliveira, M.G., Mesquita, E.D.D., Rauwerdink, A., et al. (2019). Tuberculosis-associated anemia is linked to a distinct inflammatory profile that persists after initiation of antitubercular therapy. Sci. Rep. *9*, 1381. https://doi.org/10.1038/s41598-018-37860-5.

Goldberg, B., and Stern, A. (1977). The mechanism of oxidative hemolysis produced by phenylhydrazine. Mol. Pharmacol. *13*, 832–839.

Goldberg, M.A., Dunning, S.P., and Bunn, H.F. (1988). Regulation of the erythropoietin gene: evidence that the oxygen sensor is a heme protein. Science *242*, 1412–1415. https://doi.org/10.1126/science.2849206.

Goodnough, L.T., Skikne, B., and Brugnara, C. (2000). Erythropoietin, iron, and erythropoiesis. Blood *96*, 823–833. https://doi.org/10.1182/blood.V96.3.823.

Grattagliano, I., Russmann, S., Palmieri, V.O., Portincasa, P., Palasciano, G., and Lauterburg, B.H. (2005). Glutathione peroxidase, thioredoxin, and membrane protein changes in erythrocytes predict ribavirin-induced anemia. Clin. Pharmacol. Ther. *78*, 422–432. https://doi.org/10.1016/j.clpt.2005.07.002.

Hajjar, D.P., and Gotto, A.M., Jr. (2013). Biological relevance of inflammation and oxidative stress in the pathogenesis of arterial diseases. Am. J. Pathol. *182*, 1474–1481. https://doi.org/10.1016/j.ajpath.2013.01.010.

Hanudel, M.R., Chua, K., Rappaport, M., Gabayan, V., Valore, E., Goltzman, D., Ganz, T., Nemeth, E., and Salusky, I.B. (2016). Effects of dietary iron intake and chronic kidney disease on fibroblast growth factor 23 metabolism in wild-type and hepcidin knockout mice. Am. J. Physiol. Renal Physiol. *311*, F1369–F1377. https://doi.org/10.1152/ajprenal.00281.2016.

Hara, H., and Ogawa, M. (1976). Erthropoietic precursors in mice with phenylhydrazine-induced anemia. Am. J. Hematol. *1*, 453–458. https://doi.org/10.1002/ajh.2830010410.

Hu, D., Li, D., Liu, X., Zhou, Z., Tang, J., and Shen, Y. (2020). Vanadium-based nanomaterials for cancer diagnosis and treatment. Biomed. Mater. *16*, 014101. https://doi.org/10.1088/1748-605X/abb523.

Hu, W., Zhang, Y., Jiang, Z., Wang, L., Li, J., Chen, S., Dai, N., and Si, J. (2016). The tumor promoting roles of erythropoietin/erythropoietin receptor signaling pathway in gastric cancer. Tumour Biol. *37*, 11523–11533. https://doi.org/10.1007/s13277-016-5053-7.

Huang, L.E., Ho, V., Arany, Z., Krainc, D., Galson, D., Tendler, D., Livingston, D.M., and Bunn, H.F. (1997). Erythropoietin gene regulation depends on heme-dependent oxygen sensing and assembly of interacting transcription factors. Kidney Int. *51*, 548–552. https://doi.org/10.1038/ki.1997.76.

Itano, H.A., Hirota, K., and Hosokawa, K. (1975). Mechanism of induction of haemolytic anaemia

by phenylhydrazine. Nature *256*, 665–667. https://doi.org/10.1038/256665a0.

Kaitha, S., Bashir, M., and Ali, T. (2015). Iron deficiency anemia in inflammatory bowel disease. World J. Gastrointest. Pathophysiol. *6*, 62–72. https://doi.org/10.4291/wjgp.v6.i3.62.

Kamisah, Y., Lim, J.J., Lim, C.L., and Asmadi, A.Y. (2014). Inhibitory effects of palm tocotrienol-rich fraction supplementation on bilirubin-metabolizing enzymes in hyperbilirubinemic adult rats. PLoS One *9*, e89248. https://doi.org/10.1371/journal.pone.0089248.

Kim, A., Fung, E., Parikh, S.G., Gabayan, V., Nemeth, E., and Ganz, T. (2016). Isocitrate treatment of acute anemia of inflammation in a mouse model. Blood Cells Mol. Dis. *56*, 31–36. https://doi.org/10.1016/j.bcmd.2015.09.007.

Lee, H.W., Kim, H., Ryuk, J.A., Kil, K.J., and Ko, B.S. (2014). Hemopoietic effect of extracts from constituent herbal medicines of Samul-tang on phenylhydrazine-induced hemolytic anemia in rats. Int. J. Clin. Exp. Pathol. *7*, 6179–6185.

Lippi, G., Franchini, M., and Favaloro, E.J. (2010). Thrombotic complications of erythropoiesis-stimulating agents. Semin. Thromb. Hemost. *36*, 537–549. https://doi.org/10.1055/s-0030-1255448.

Locatelli, F., Fishbane, S., Block, G.A., and Macdougall, I.C. (2017). Targeting hypoxia-inducible factors for the treatment of anemia in chronic kidney disease patients. Am. J. Nephrol. *45*, 187–199. https://doi.org/10.1159/000455166.

Macdougall, I.C. (2012). New anemia therapies: translating novel strategies from bench to bedside. Am. J. Kidney Dis. *59*, 444–451. https://doi.org/10.1053/j.ajkd.2011.11.013.

Mcbride, J.A., and Striker, R. (2017). Imbalance in the game of T cells: what can the CD4/CD8 T-cell ratio tell us about HIV and health? PLoS Pathog. *13*, e1006624. https://doi.org/10.1371/journal.ppat.1006624.

Means, R.T., Jr. (1994). Clinical application of recombinant erythropoietin in the anemia of chronic disease. Hematol. Oncol. Clin. North. Am. *8*, 933–944.

Mittal, M., Siddiqui, M.R., Tran, K., Reddy, S.P., and Malik, A.B. (2014). Reactive oxygen species in inflammation and tissue injury. Antioxid. Redox. Signal. *20*, 1126–1167. https://doi.org/10.1089/ars.2012.5149.

Murphy, M.F., Estcourt, L., and Goodnough, L.T. (2017). Blood transfusion strategies in elderly patients. Lancet Haematol. *4*, e453–e454. https://doi.org/10.1016/S2352-3026(17)30173-4.

Naughton, B.A., Dornfest, B.S., Bush, M.E., Carlson, C.A., and Lapin, D.M. (1990). Immune activation is associated with phenylhydrazine-induced anemia in the rat. J. Lab. Clin. Med. *116*, 498–507.

Nguyen, P.H., Scott, S., Avula, R., Tran, L.M., and Menon, P. (2018). Trends and drivers of change in the prevalence of anaemia among 1 million women and children in India, 2006 to 2016. BMJ Glob. Health *3*, e001010. https://doi.org/10.1136/bmjgh-2018-001010.

Nguyen, T.L., and Duran, R.V. (2016). Prolyl hydroxylase domain enzymes and their role in cell signaling and cancer metabolism. Int. J. Biochem. Cell Biol. *80*, 71–80. https://doi.org/10.1016/j.biocel.2016.09.026.

Niki, E. (2008). Lipid peroxidation products as oxidative stress biomarkers. Biofactors *34*, 171–180. https://doi.org/10.1002/biof.5520340208.

Nyakundi, B.B., Toth, A., Balogh, E., Nagy, B., Erdei, J., Ryffel, B., Paragh, G., Cordero, M.D., and Jeney, V. (2019). Oxidized hemoglobin forms contribute to NLRP3 inflammasome-driven IL-1beta production upon intravascular hemolysis. Biochim. Biophys. Acta, Mol. Basis Dis. *1865*, 464–475. https://doi.org/10.1016/j.bbadis.2018.10.030.

Opasich, C., Cazzola, M., Scelsi, L., De Feo, S., Bosimini, E., Lagioia, R., Febo, O., Ferrari, R., Fucili, A., Moratti, R., et al. (2005). Blunted erythropoietin production and defective iron supply for erythropoiesis as major causes of anaemia in patients with chronic heart failure. Eur. Heart J. *26*, 2232–2237. https://doi.org/10.1093/eurheartj/ehi388.

Pasricha, S.R., Tye-Din, J., Muckenthaler, M.U., and Swinkels, D.W. (2021). Iron deficiency. Lancet *397*, 233–248. https://doi.org/10.1016/S0140-6736(20)32594-0.

Patwari, J., Chatterjee, A., Sardar, S., Lemmens, P., and Pal, S.K. (2018). Ultrafast dynamics in co-sensitized photocatalysts under visible and NIR light irradiation. Phys. Chem. Chem. Phys. *20*, 10418–10429. https://doi.org/10.1039/C7CP08431E.

Paulson, R.F. (2014). Targeting a new regulator of erythropoiesis to alleviate anemia. Nat. Med. *20*, 334–335. https://doi.org/10.1038/nm.3524.

Paulson, R.F., Shi, L., and Wu, D.C. (2011). Stress erythropoiesis: new signals and new stress progenitor cells. Curr. Opin. Hematol. *18*, 139–145. https://doi.org/10.1097/MOH.0b013e32834521c8.

Puthenparambil, J., Lechner, K., and Kornek, G. (2010). Autoimmune hemolytic anemia as a paraneoplastic phenomenon in solid tumors: a critical analysis of 52 cases reported in the literature. Wien Klin. Wochenschr. *122*, 229–236. https://doi.org/10.1007/s00508-010-1319-z.

Richardson, C.L., Delehanty, L.L., Bullock, G.C., Rival, C.M., Tung, K.S., Kimpel, D.L., Gardenghi, S., Rivella, S., and Goldfarb, A.N. (2013). Isocitrate ameliorates anemia by suppressing the erythroid iron restriction response. J. Clin. Invest. *123*, 3614–3623. https://doi.org/10.1172/JCI68487.

Rokushima, M., Omi, K., Imura, K., Araki, A., Furukawa, N., Itoh, F., Miyazaki, M., Yamamoto, J., Rokushima, M., Okada, M., et al. (2007). Toxicogenomics of drug-induced hemolytic anemia by analyzing gene expression profiles in the spleen. Toxicol. Sci. *100*, 290–302. https://doi.org/10.1093/toxsci/kfm216.

Sankaran, V.G., and Weiss, M.J. (2015). Anemia: progress in molecular mechanisms and therapies. Nat. Med. *21*, 221–230. https://doi.org/10.1038/nm.3814.

Schaer, D.J., Buehler, P.W., Alayash, A.I., Belcher, J.D., and Vercellotti, G.M. (2013). Hemolysis and free hemoglobin revisited: exploring hemoglobin and hemin scavengers as a novel class of therapeutic proteins. Blood *121*, 1276–1284. https://doi.org/10.1182/blood-2012-11-451229.

Sinclair, A.M. (2013). Erythropoiesis stimulating agents: approaches to modulate activity. Biologics *7*, 161–174. https://doi.org/10.2147/BTT.S45971.

Song, S.N., Iwahashi, M., Tomosugi, N., Uno, K., Yamana, J., Yamana, S., Isobe, T., Ito, H., Kawabata, H., and Yoshizaki, K. (2013). Comparative evaluation of the effects of treatment with tocilizumab and TNF-alpha inhibitors on serum hepcidin, anemia response and disease activity in rheumatoid arthritis patients. Arthritis Res. Ther. *15*, R141. https://doi.org/10.1186/ar4323.

Sparkenbaugh, E.M., Chantrathammachart, P., Wang, S., Jonas, W., Kirchhofer, D., Gailani, D., Gruber, A., Kasthuri, R., Key, N.S., Mackman, N., and Pawlinski, R. (2015). Excess of heme induces tissue factor-dependent activation of coagulation in mice. Haematologica *100*, 308–314. https://doi.org/10.3324/haematol.2014.114728.

Spivak, J.L., Toretti, D., and Dickerman, H.W. (1973). Effect of phenylhydrazine-induced hemolytic anemia on nuclear RNA polymerase activity of the mouse spleen. Blood *42*, 257–266. https://doi.org/10.1182/blood.V42.2.257.257.

Suragani, R.N., Cadena, S.M., Cawley, S.M., Sako, D., Mitchell, D., Li, R., Davies, M.V., Alexander, M.J., Devine, M., Loveday, K.S., et al. (2014). Transforming growth factor-beta superfamily ligand trap ACE-536 corrects anemia by promoting late-stage erythropoiesis. Nat. Med. *20*, 408–414. https://doi.org/10.1038/nm.3512.

Theurl, I., Hilgendorf, I., Nairz, M., Tymoszuk, P., Haschka, D., Asshoff, M., He, S., Gerhardt, L.M., Holderried, T.A., Seifert, M., et al. (2016). On-demand erythrocyte disposal and iron recycling requires transient macrophages in the liver. Nat. Med. *22*, 945–951. https://doi.org/10.1038/nm.4146.

Thomas, M.C. (2007). Anemia in diabetes: marker or mediator of microvascular disease? Nat. Clin. Pract. Nephrol. *3*, 20–30. https://doi.org/10.1038/ncpneph0378.

Thomas, M.C., Tsalamandris, C., Macisaac, R., Medley, T., Kingwell, B., Cooper, M.E., and Jerums, G. (2004). Low-molecular-weight AGEs are associated with GFR and anemia in patients with type 2 diabetes. Kidney Int. *66*, 1167–1172. https://doi.org/10.1111/j.1523-1755.2004.00868.x.

Tolosano, E., Fagoonee, S., Hirsch, E., Berger, F.G., Baumann, H., Silengo, L., and Altruda, F. (2002). Enhanced splenomegaly and severe liver inflammation in haptoglobin/hemopexin double-null mice after acute hemolysis. Blood *100*, 4201–4208. https://doi.org/10.1182/blood-2002-04-1270.

Tribe, C.R. (1973). A comparison of rapid methods including imprint cytodiagnosis for the

diagnosis of breast tumours. J. Clin. Pathol. *26*, 273–277. https://doi.org/10.1136/jcp.26.4.273.

Wagener, F.A., Eggert, A., Boerman, O.C., Oyen, W.J., Verhofstad, A., Abraham, N.G., Adema, G., Van Kooyk, Y., De Witte, T., and Figdor, C.G. (2001). Heme is a potent inducer of inflammation in mice and is counteracted by heme oxygenase. Blood *98*, 1802–1811. https://doi.org/10.1182/blood.V98.6.1802.

Wang, H., Liu, D., Song, P., Jiang, F., Chi, X., and Zhang, T. (2021). Exposure to hypoxia causes stress erythropoiesis and downregulates immune response genes in spleen of mice. BMC Genom. *22*, 413. https://doi.org/10.1186/s12864-021-07731-x.

Weiss, G., and Goodnough, L.T. (2005). Anemia of chronic disease. N. Engl. J. Med. *352*, 1011–1023. https://doi.org/10.1056/NEJMra041809.

Wikby, A., Ferguson, F., Forsey, R., Thompson, J., Strindhall, J., Lofgren, S., Nilsson, B.O., Ernerudh, J., Pawelec, G., and Johansson, B. (2005). An immune risk phenotype, cognitive impairment, and survival in very late life: impact of allostatic load in Swedish octogenarian and nonagenarian humans. J. Gerontol. A. Biol. Sci. Med. Sci. *60*, 556–565. https://doi.org/10.1093/gerona/60.5.556.

Wrighton, N.C., Farrell, F.X., Chang, R., Kashyap, A.K., Barbone, F.P., Mulcahy, L.S., Johnson, D.L., Barrett, R.W., Jolliffe, L.K., and Dower, W.J. (1996). Small peptides as potent mimetics of the protein hormone erythropoietin. Science *273*, 458–464. https://doi.org/10.1126/science.273.5274.458.

Zhang, B., Yan, W., Zhu, Y., Yang, W., Le, W., Chen, B., Zhu, R., and Cheng, L. (2018). Nanomaterials in neural-stem-cell-mediated regenerative medicine: imaging and treatment of neurological diseases. Adv. Mater. *30*, e1705694. https://doi.org/10.1002/adma.201705694.

Zhao, B., Mei, Y., Yang, J., and Ji, P. (2016). Erythropoietin-regulated oxidative stress negatively affects enucleation during terminal erythropoiesis. Exp. Hematol. *44*, 975–981. https://doi.org/10.1016/j.exphem.2016.06.249.

STAR★METHODS

KEY RESOURCES TABLE

REAGENT or RESOURCE	SOURCE	IDENTIFIER
Antibodies		
CD3e Hamster anti-Mouse, FITC, Clone: 145-2C11, BD	BD Biosciences	Cat. No: BDB561827
CD4 Rat anti-Mouse, PE-Cy7, Clone: RM4-5, BD	BD Biosciences	Cat. No: BDB561099
CD8a Rat anti-Mouse, APC-H7, Clone: 53-6.7, BD	BD Biosciences	Cat. No: BDB560247
CD18 Rat anti-Mouse, PE, Clone: C71/16, BD	BD Biosciences	Cat. No: BDB553293
CD45 Rat anti-Mouse, PerCP-Cy5.5, Clone: 30-F11, BD	BD Biosciences	Cat. No: BDB561869
CD19 Rat anti-Mouse, APC, Clone: 1D3, BD	BD Biosciences	Cat. No: BDB561738
Chemicals, peptides, and recombinant proteins		
Phenylhydrazine	Sigma-Aldrich	P26252; CAS: 100-63-0
Manganese chloride tetrahydrate	Sigma-Aldrich	63535; CAS: 13446-34-9
Citric acid monohydrate	Sigma-Aldrich	C7129; CAS: 5949-29-1
2′,7′-dichlorofluorescein diacetate	Sigma-Aldrich	D6883; CAS: 4091-99-0
Hematoporphyrin	Sigma-Aldrich	H5518; CAS: 14459-29-1
Critical commercial assays		
Mouse EPO Elisa Kit	Elabscience	Cat. No:E-EL-M3058
SOD Assay Kit	Sigma-Aldrich	Product No: 19160; SKU: 19160-1KT-F
Catalase Assay Kit	Sigma-Aldrich	Product No: CAT100; SKU: CAT100-1KT
Glutathione Peroxidase Assay Kit	Sigma-Aldrich	Product No: MAK437; SKU: MAK437-1KT
Experimental models: Organisms/strains		
C57BL/6J Mouse	Saha Enterprise, India	NA
Software and algorithms		
Prism-GraphPad	GraphPad Software	https://www.graphpad.com/scientific-software/prism/
SigmaPlot	SYSTAT	https://systatsoftware.com/sigmaplot/

RESOURCE AVAILABILITY

Lead contact

Further information and requests for resources and reagents should be directed to and will be fulfilled by the lead contact, S.K.P (skpal@bose.res.in).

Materials availability

The authors confirm that the materials are available from the lead contact, S.K.P (skpal@bose.res.in), upon reasonable request.

Data and code availability

- All data reported in this paper will be shared by the lead contact upon request.
- This paper does not report original code.
- Any additional information required to reanalyze the data reported in this paper is available from the lead contact upon request.

EXPERIMENTAL MODEL AND SUBJECT DETAILS

Rodent model

All animal studies and experimental procedures were performed at Central Animal Facility, Dept. of Zoology, Uluberia College, India (Reg. No.: 2057/GO/ReRcBi/S/19/CPCSEA) following the protocol approved by the Institutional Animal Ethics Committee (IAEC) as per standard guideline of Committee for the Purpose of Control and Supervision of Experiments on Animals (CPCSEA), Ministry of Fisheries, Animal Husbandry and Dairying, Govt. of India. Nonanemic C57BL/6J mice of both sexes (age: 2–3 weeks, body weight, BW: 22 $\pm$ 2.45 g) were used in the current study. Animals were housed under specific-pathogen-free (SPF) conditions (maximum 5 mice per polypropylene cage; temp: 25 $\pm$ 2.0°C; ~55%–60% relative humidity) under a 12-h light and 12-h dark cycle with access to food (standard chow for mice, Saha Enterprise, India) and water *ad libitum*. Autoclaved nest material and paper houses served as cage enrichment for mice. Before the experiment all the animals kept 10 days for acclimatization. Animal cages were always randomly assigned to treatment or control groups.

METHOD DETAILS

Materials

Manganese chloride tetrahydrate, Citric acid monohydrate, Sodium hydroxide, Phenylhydrazine, 2′,7′-dichlorofluorescein diacetate (DCFH-DA), Hematoporphyrin were purchased from Sigma-Aldrich (St Louis, MO, USA). All other chemicals were acquired from Sigma Aldrich (St Louis, MO, USA) unless otherwise stated. Whenever required milli pore water was used.

Synthesis of Mn-citrate NC

1.98 gm of manganese chloride ($MnCl_2$) salt (1M) and 2.10 gm of citric acid monohydrate (1M) was dissolved in 10 mL Milli. Q water. Then the mixture was heated at 45°C water bath for 15 min under continuous stirring. After that, aqueous solution of sodium hydroxide (NaOH; 4M) was added to the heated solution. The pH of the new mixture should be 7. Then this mixture was heated at 65°C water bath for 15 min under continuous stirring. Next, the solution was kept in a water bath at 60°C without any stirring until it turned to light brown color. The supernatant is discarded and the precipitate was washed three times with ethanol. Remaining ethanol was evaporated and the dry crystalline sample of Manganese-citrate nano-complex is obtained. The dry sample was dispersed in water for further studies (Patent Reference Number: 202131034977) related to Mn-citrate NC.

Characterization techniques

Images of HRTEM and transmission electron microscope (TEM) were obtained using a FEI TecnaiTF-20 field emission HRTEM operating at 200 kV. For the preparation of TEM sample, the nanocomplex solution was drop-casted on a 300-mesh amorphous carbon-coated copper grid and kept overnight at ambient temperature. The X-ray diffraction (XRD) patterns of the samples were obtained using a Panalytical XPERT PRO diffractometer equipped with Cu Kα radiation (at 40 mA and 40 kV) by using a scanning rate of 0.021 S^{-1} in the 2θ range from 201 to 801. Using Shimadzu UV-Vis 2600 spectrometer absorbance spectra of Mn-citrate NCs were measured. Fluorescence excitation and emission spectra of the prepared nanoparticle was accessed using Fluorolog, Model LFI-3751 (Horiba-JobinYvon, Edison, NJ) spectrofluorimeter. We followed the methodologies for picosecond resolved spectroscopic analysis reported in our previous studies.

Study design

The purpose of this study was to assess the potential of orally-administrable manganese citrate nano-complex (Mn-citrate NC) as a prophylactic as well as a therapeutic agent for rapid recovery from anemia of inflammation and anemia in general. We performed detailed physicochemical characterization of Mn-citrate NC by TEM, HRTEM, XRD, Photoluminescence spectroscopy etc. To define *in vivo* effects of Mn-citrate NC, we selected C57BL/6J mice as our preclinical animal model.

The *in vivo* study was conducted in two phases. In the first phase, the prophylactic role of Mn-Citrate NC against development and progression of anemia was evaluated along with antioxidant enzyme activity and inflammatory cytokines level. And hemoglobin level and RBCs count was monitored in time dependent manner. In the second phase, the therapeutic potential of Mn-citrate NC in treatment of anemia was assessed.

Phase 1

Mice were randomly divided into five groups (N = 10/group). Animals of Group 1 served as control and received normal saline (150 μL; oral). Animals of Group 2 served as diseased model and received single dose (intraperitoneal injection) of PHz; 60 mg kg^{-1} BW at day 0. Animals of Group 3 received single dose (i.p.inection) of PHz; 60 mg kg^{-1} BW and single oral dose of Mn-citrate NC (0.25 mg kg^{-1} BW) at day 0. Animals of Group 4 served as NC control and received single oral dose of Mn-citrate NC (0.25 mg kg^{-1} BW) at day 0. And animals of Group 5 received single oral dose of citrate (0.15 mg kg^{-1} BW) at day 0. All doses were finalized based on reported literature and pilot experimentation.

Phase 2

Animals were randomly divided into five groups (N = 10/group). Animals of Group 1 served as control and received normal saline (150 μL; oral). Animals of Group 2 served as diseased model and received single dose (intraperitoneal injection) of PHz; 60 mg kg-^{1} BW at day 0. Animals of Group 3 received single dose (intraperitoneal injection) of PHz; 60 mg kg^{-1} BW at day 0. Animals of Group 4 served as NC control and received single oral dose of Mn-citrate NC (0.25 mg kg^{-1} BW) at day 4. And animals of Group 5 received single dose (intraperitoneal injection) of PHz; 60 mg kg^{-1} BW at day 0. After development of severe anemia on day 4, Group 2 animals left untreated, Group 3 animals received single oral dose of Mn-citrate NC (0.25 mg kg^{-1} BW), animals of Group 5 received single oral dose of citrate (0.15 mg kg^{-1} BW). All doses were finalized based on reported literature and pilot experimentation.

Dosing description

Phenylhydrazine was administrated intraperitoneally and the Mn-citrate NC (nano-ESA) was administrated orally in this study. In case of PHz, we have used disposable syringe for intraperitoneal injection. And we have used gavage needles for orally administration of Mn-citrate NC. In case of phase 1 study, we have administrated PHz (intraperotoneally) and nano-ESA (orally) one after another. And in phase 2 study, we have administrated nano-ESA (orally) after 4 days of PHz administration (intraperotoneally).

Induction of anemia

We used well known phenylhydrazine (PHz) intoxication model with slight modifications (Spivak et al., 1973; Goldberg and Stern, 1977; Itano et al., 1975; Naughton et al., 1990). It causes severe hemolysis i.e. abnormal breakdown of RBCs rapidly and also induces inflammation and oxidative stress, in turn, stimulates a pathophysiological condition of anemia of inflammation (Naughton et al., 1990).

Measurement of hemoglobin concentration

Small amount of blood samples (20 ul) were collected from tail vein of each mouse for each time point at regular intervals. And then the concentration of hemoglobin in blood was estimated using commercially available test kits (HEMOCOR-D, Tulip Diagonosticspvt. Ltd, Uttarakhand, India) following the protocols suggested by the corresponding manufacturers.

Blood collection

At the end of the experimental period, the animals were euthanized and decapitated after being fasted. Blood was collected from retro orbital plexus just before sacrifice, kept in sterile non-heparinized tubes for further analysis.

Assessment of hematological parameters

For hematological studies, the blood was collected in heparinized tubes. Blood-cell count was done using blood smears in Sysmax-K1000 Cell Counter. Parameters studied were hemoglobin, total red blood cells, hematocrit, packed cell volume (PCV), mean corpuscular volume (MCV), mean corpuscular hemoglobin (MCH), mean corpuscular hemoglobin concentration (MCHC), platelets, total white blood cells etc.

Blood film preparation and staining

A small drop of blood was placed on the pre-cleaned, labeled slide, near its frosted end. Another slide was brought at a 30–45° angle up to the drop, allowing the drop to spread along the contact line of the 2 slides. Quickly push the upper (spreader) slide toward the unfrosted end of the lower slide. Then the blood film was rapidly air dried. Now, the film was covered with Leishman's Stain and allowed to act for 2 min.

Methanol in the stain fixed the preparation. After that double volume of distilled water was added to the slide and mixed well. The diluted stain was allowed to act for 10–15 min. Finally, the film was washed with phosphate buffer of pH 7.0, drained and well dried in air for examination under the microscope (Dewinter Classic of Milano, Italy) equipped with a CCD based camera.

Evaluation of osmotic resistance of RBCs

The osmotic resistance of red blood cells was evaluated according to the method described early by Redondo et al. The method consists to induce the lysis of red blood cell in hypotonic solution. For this study, the procedure used is as follow: a range of saline solution from 0% to 0.9% is prepared and 50 μL of blood were mixed with each saline solution. The mixture is shaking slightly and incubated for 60 min. After the incubation, the mixture is centrifuged at 1085 rpm for 10 min. The supernatant is collected and the absorbance is determined at 540 nm with spectrophotometer (Double Beam Spectrophotometer UH5300, HITACHI). The percentage of haemolysis is determined by the ratio absorbance test/absorbance full haemolysis. It is suggested that the full haemolysis is occurred in the distilled water. Haemolysis curve is generated in function of sodium chloride concentration.

Histopathological examination

At the end of the experimental period, the animals were sacrificed and spleens were collected for histopathological examination. For microscopic evaluation, a conventional technique of paraffin wax sectioning and differential staining was used (Adhikari et al., 2018). Tissues are fixed with neutral formalin 10%, embedded in paraffin, and then manually sectioned with a microtome to obtain 4-5 μm-thick paraffin sections. Microtome was used to prepare ultrathin sections (4–5 μm), followed by staining with hematoxylin and eosin (H and E) and silver stain. Histopathological changes were examined under the microscope (Dewinter Classic of Milano, Italy) equipped with a CCD based camera. We also prepared touch preparation of spleen on a glass slide. After sectioning of the freshly collected spleen, the tissue was carefully touched with sterilized blotting paper to soak the blood on the surface. Then glass slides were gently touched on the cut surface of the tissue to get imprint smear on the slide. Imprint smears were immediately fixed in 95% alcohol and stained with Leishman's Stain and Perls' Prussian blue stain (Tribe, 1973).

Cell preparation and flow cytometry analysis

At the end of the experimental period, the animals were sacrificed and spleens were collected and harvested aseptically. Next, the tissue was gently smashed between two microscopic glass slides and filtered through cell strainers to prepare single cell suspension. After lysis of RBCs, suspension was washed with sterilized PBS. And this washing step was repeated for 3 times. Finally, the cell concentration of the suspension was adjusted to a concentration of 1.0×10^7/mL for flow cytometry analysis. Now, the prepared cell suspension was incubated with required volume of each of the fluorescently labeled antibodies for 30 min at 4°C to detect lymphocyte subgroups. Before analysis, solution is washed three times with PBS. The stained cells were then analyzed by flow cytometry immediately (FC500, Beckman, USA). Fluorescently labeled antibodies included FITC-conjugated anti-CD3e, PE-Cy7 conjugated anti-CD4, APC-H7 conjugated anti-CD8a, PE conjugated anti-CD18, PerCP-Cy 5.5 conjugated CD45, and APC conjugated anti-CD19 (BD Biosciences, USA).

RBC hemolysate preparation

The collected blood was then centrifuged at 3000 g for 10 min at 4°C. The supernatant plasma was removed and packed red blood cells (RBCs) were resuspended in PBS (0.1 M, pH 7.4). The cell suspension was then washed thrice and the supernatant aspirated. For hemolysate preparation, 1 part of fresh packed RBCs was added with 9 part of ice-cold distilled water and shaken gently. Prepared RBC hemolysate was used for biochemical analysis (Kamisah et al., 2014).

Assessment of lipid peroxidation and antioxidant enzyme activity

The RBC hemolysates were used to determine the activity of SOD, CAT and GPx as well as the content of MDA. SOD, CAT and GPx activities were estimated using commercially available test kits (Sigma-Aldrich, MO, USA) following the protocols described by the manufacturer. To assess the extent of lipid peroxidation, the level of malonyldialdehyde (MDA), a substance that reacts with thiobarbituric acid, was determined in the RBC hemolysates according to the method of Grattagliano et al. (2005). These parameters were measured on day 4 of phase 1 study.

Serum isolation

After collection of blood, kept in sterile non-heparinized tubes in slanting position at 45° angle for 45 min and centrifuged at 3500×g for 20 min. The clear serum (straw color) was obtained and used in subsequent biochemical analysis.

Measurement of erythropoietin and inflammatory cytokines level

All serum samples were sterile, hemolysis-free and were stored at −20°C before determination of the biochemical parameters. The concentration of EPO in serum was determined using commercially available test kits (Mouse EPO ELISA Kit, Elabscience, USA) following the protocols described by the corresponding manufacturers. And inflammatory cytokines (TNF-α, IFN-γ, IL-6, IL-1β, and IL-10) were measured according to the respective protocol provided by kit manufacturers. These parameters were measured on different time points throughout the study.

Evaluation of interaction of Mn-citrate NC with the porphyrin rings of hematoporphyrin

To study the incorporation of Mn-citrate NC within the porphyrin rings, steady state fluorescence spectra-were recorded with JobinYvon Fluorologfluorimeter, using an excitation wavelength of 409 nm. Time-resolved fluorescence transients were recorded using LifeSpec-ps, Edinburgh Instruments, UK equipped with a micro channel plate photomultiplier tube. The excitation wavelength for all the experiments was kept at 410 nm. A 1mM stock solution of hematoporphyrin was prepared and the incorporation of the NC was studied by subsequent addition of the Mn-Citrate NC to thehematoporphyrin solution, followed by overnight stirring.

QUANTIFICATION AND STATISTICAL ANALYSIS

All quantitative data are expressed as Mean ± SD unless otherwise stated. One-way ANOVA followed by correction of false discovery rate (post hoc FDR: two stage step up method of Benjamini, Krieger and Yekutieli) for multiple comparisons was performed for comparison between multiple groups (Benjamini et al., 2006). Beforehand, the normality of each parameter was checked by normal quantile–quantile plots. Sample size in our animal studies were determined following the standard sample sizes previously been used in similar experiments as per relevant literature. Designated sample size (in figure legends) always refers to biological replicates (independent animals). GraphPad Prism v8.0 (GraphPad Software), and Sigmaplot v14.0 (Systat Software, Inc.) were used for statistical analysis. For all comparisons, a p value < 0.05 was considered to be statistically significant.